UiT The Arctic University of Norway

Faculty of Health Sciences

Mutational drivers of a dysfunctional local immune response in resected non-small cell lung cancer (NSCLC) patients

Master thesis in Medicine (MED-3950), June 2023

Author: Patrick Holmstad
Primary Supervisor: Mehrdad Rakaee, PhD; Department of Clinical Medicine, Faculty of Health Sciences, UiT

Secondary Supervisor: Elin Richardsen, MD, PhD; Department of Clinical Pathology, University Hospital of North Norway
Secondary Supervisor: Tom Dønnem, MD, PhD; Department of Clinical Medicine, Faculty of Health Sciences, UiT

Acknowledgement

The research documented in this thesis was conducted at the Translational Cancer Research Group, UiT Arctic University of Norway, and in collaboration with the Department of Clinical Pathology at UNN. The work was supervised by Dr. Mehrdad Rakaee, Prof. Elin Richardsen and Prof. Tom Dønnem. I would like to express my great appreciation for the work and time that you have put into guiding me. I would especially like to thank Elin for introducing me to the research group and the people involved. She has been very supportive and patient with me.

I would like to say a big thank you to all the patients who have agreed to participate in the research project, and without their participation, none of this would have been possible.

I would also like to thank Marte Berglund and the other lab technicians at the Molecular Pathology laboratory, UNN, who have carried out the NanoString analysis, taught me how to perform them and finally made the samples themselves user-friendly.

Finally, I would like to thank Erlend and my friends, who have provided moral support throughout the whole project.

Patrick Holmstad, May 2023

Table of contents

Summary

Background: Patients with KEAP1 and STK11 alterations have shown poor response to immunotherapy in non-small cell lung cancer (NSCLC) due to unknown underlying mechanisms. In a sub-study of the TNM-I trial (NCT03299478), we discovered that lung adenocarcinomas (LUAD) with concurrent KEAP1 and STK11 mutations exhibit predominantly non-inflamed immunological features, potentially contributing to immunotherapy resistance (PMID: 37100205). However, it is unclear whether single mutations or co-mutations drive this phenomenon.

Methods: Among 215 patients (stage I-IIIA) who underwent genomic profiling, tumor tissue from 23 LUAD patients with STK11 and KEAP1 mutations were included in this thesis. NanoString gene expression analysis with the nCounter PanCancer IO 360™ Panel was performed and analyzed. Comparisons of gene expression and metagene changes were assessed across single versus co-mutations.

Results: 44% (n = 10) of the cohort had co-mutations, while 56% (n = 13) had a single mutation with either KEAP1 or STK11. In STK11 vs co-mutation, pathway analysis revealed up-regulation of genes associated with adaptive immunity. Specifically, B cells were generally upregulated (p-adj < 0.05) in STK11 altered cases. In KEAP1 vs co-mutation, matrix remodeling and metastasis pathways were highly enriched, with the highest fold changes for MMP7 and MMP9 (5.19, 3.34, respectively; p-adj < 0.05). Additionally, we found up-regulation of chemoresistant pathways in KEAP1 mutated patients (p-adj < 0.05). In STK11 vs KEAP1, NF-kappaB was the most altered pathway.

Conclusion: KEAP1 mutation is the main driver of the non-inflamed phenotype in LUAD compared to STK11 mutation, and it contributes to a more aggressive disease through activation of metastatic pathways and chemoresistance features. These results need to be validated in larger datasets.

Abbreviations

ALK – Anaplastic lymphoma kinase
AMPK – AMP-activated protein kinase
BRAF – V-raf murine sarcoma viral oncogene homolog B1
CCI – Charlson Comorbidity Index
CT – Computed Tomography Scan
cTNM – Clinical tumor (T), nodes (N), and metastases (M)
dGSS – Directed Global Significance Score
dsDNA – Double-stranded DNA
EGFR – Epidermal growth factor receptor
ES – Enrichment score
FC – Fold change
FDR – False discovery rates
FOV – Fields of view
GES – Gene expression signatures
GO – Gene ontology
GSA – Gene set analysis
GSEA – Gene set enrichment analysis
GSS – Global Significance Score
HER – Human epidermal growth factor
ICIs – Immune checkpoint inhibitors
IHC – Immunohistochemistry
IPM – Intrapulmonary metastasis
IRB – Institutional Review Board
KEAP1 – Kelch-like ECH-associated protein 1
KRAS – Kirsten rat sarcoma viral oncogene homologue
LCNEC – Large cell neuroendocrine carcinoma
LKIB1 – Liver kinase B1
MDSCs - Myeloid-derived suppressor cells
MDT – Multidisciplinary teams meeting
MMP – Matrix metalloproteinase
mRNA – messenger RNA
mTOR – Mammalian target of rapamycin
NADH – Nicotinamide adenine dinucleotide with hydrogen
NF-κB – Nuclear factor kappa-light-chain-enhancer of activated B cells
NFE2L2 – Nuclear factor erythroid-2-related factor 2
NRF2 – Nuclear factor erythroid 2-related factor 2
NSCLC – Non-small celled lung cancer
NTRK – Neurotrophic Tyrosine Receptor Kinaseand
PD-L1 – Programmed death-ligand 1
PD1 – Programmed death receptor 1
PI3K – Phosphatidylinositol 3-kinase
PLC – Primary lung cancer
REK - Regional Committee
ROS1 – Receptor tyrosine kinase-like orphan receptor 1
SCLC – Small celled lung cancer
STING – Stimulator of interferon gene
STK11 - Serine/threonine kinase 11
TAMs – Tumor Associated Macrophages
TBK1 – Tank-binding kinase 1
TNM – Tumor (T), nodes (N), and metastases (M)
TNM-I – Tumor–node–metastasis – Immunoscore

1 Introduction to lung cancer

1.1 Epidemiology

Lung cancer is today the most common form of cancer in the world in both women and men, while at the same time being the leading cause of cancer related death (1). This is also seen in Norway, where lung cancer is the second most frequent form of cancer in both women and men (2). In the diagnosis year 2022, 3,466 new cases of lung cancer were registered in Norway, where an almost equal number of women and men were diagnosed (3). The median age for lung cancer is 73 years for both sexes, which means that half of all those diagnosed are over 73 years old (3). See **Figure S1** (supplementary data) for an overview of incidence by gender and age groups between 1992-2022 (3). Compared to previous years, this is actually only a modest increase, despite the fact that this is the highest incidence ever recorded (in 2021, the number of newly diagnosed cases was 3,422) (2, 3). But in general there has been a flattening incidence since 2018 in Norway, where the situation now is such that there is a decreasing incidence for those < 70 years and a flattening incidence for those > 70+ years (**Figure S1)** (3).

Despite the fact that there never have been more people diagnosed with lung cancer than today, the good news is that there has been a reduction in mortality from lung cancer over the last 20 years (2). **Figure S2** shows the relative 5-year survival rate for lung cancer in men and women, and how it has increased almost three times for both sexes from 1965 to 2021 (4).

1.2 Risk factors

Although it is now quite clear that smoking is the main cause of lung cancer, there are many other well-known carcinogens and risk factors (5). It is well known that people who have never so much as taken a puff of cigarette smoke can develop lung cancer, in addition to knowing that lung cancer existed before smoking became commercial (6). From earlier days it was known that people who worked in coal mines and other mining operations, not infrequently developed lung cancer (7). Today we know that, in addition to smoking; asbestos, aluminum production, radon-222 and silica dust - as well as many more agents, are carcinogens that can cause lung cancer (5, 6, 8). These substances are registered as class 1 carcinogens on the the International Agency for Research on Cancer (IARC's) list - which means that

there is sufficient evidence for carcinogenicity in humans. In other words, there is convincing evidence that the agent causes cancer in humans (8, 9).

Apart from the discussed risk factors, mutations and single-nucleotide polymorphisms are known to be associated with lung cancer (6). Meta-analyses have shown that there is a 2-fold increased risk of lung cancer in people with a family history of lung cancer in those who have not smoked (6, 10). Familial association studies have identified lung cancer associated genes with high penetrance and low frequency (6). Examples of identified genetic mutations that increase the risk of lung cancer are variations in 5p15.33 (telomerase reverse transcriptase gene), 6p21.33 (cytochrome P450 family 21 subfamily A member 2), and 15q25.1 (cholinergic receptor nicotinic alpha 5 subunit) (5, 6). Also, single-nucleotide polymorphisms at 22q12 (Checkpoint kinase 2) and the 15q15.2 (ubiquitin protein ligase E3 component) locus have been highly associated with increased risk of lung cancer (5, 6).

In addition to the aforementioned risk factors, there are a number of other factors that have been suggested to be linked to lung cancer (6, 11-19). Respiratory diseases such as chronic obstructive pulmonary disease, pneumonia, asthma, tuberculosis give an increased risk of cancer, with chronic obstructive pulmonary disease being the disease that gives the greatest risk (6). Other examples of risk factors can be improper diet, alcohol consumption, marijuana smoking, estrogen, infections with human papillomavirus, human immunodeficiency virus, and Epstein-Barr virus (6, 11-19). The latter are suggested risk factors in the literature, where there is a lack of clear evidence to ascertain their relationship (6).

1.3 Diagnosis and investigation of lung cancer in Norway

1.3.1 Guidelines for the investigation of lung cancer

In Norway, there are standardized guidelines - or in Norwegian "pakkeforløp", for lung cancer (20). Today, almost all of the most common forms of cancer have their own guidelines, where the guidelines gives patients with a justified suspicion of cancer predictability and security (20). The goal of the guidelines is to give the patient comprehensive workup and prevent unnecessary delays for diagnostics (20, 21).

The guidelines for lung cancer was introduced in Norway in 2015 (21). When a medical doctor suspects that the patient could have lung cancer, the patient is referred for further investigations in accordance with these guidelines. (20). From the time the referral is made to the first appearance in the investigating department, a maximum of 7 calendar days must have passed, and from the patient's first appearance in the department to the end of the examination, a maximum of 21 calendar days must have passed (21). In addition, there are also certain deadlines when it comes to how long it will take before the patient receives treatment. For example; if the investigation finds that the patient needs surgical treatment, a maximum of 14 calendar days must elapse from the end of the investigation to the start of treatment (21). See **Table S1** for a complete overview of the various deadlines (21). These deadlines apply to all hospitals in Norway that investigate lung cancer and all patients - regardless of geography, must have the same offer (21).

In principle, most people with lung cancer can be examined and treated at a local hospital, but because medicine is becoming more and more personalized, most people are also in contact with a larger regional hospital during treatment for their cancer. It is especially pathological diagnostics and oncological drugs and radiation that require much of the treatment carried out in the larger hospitals (22).

1.3.2 Investigation of lung cancer - general overview

When a patient is referred in accordance to the guidelines for lung cancer, it is first and foremost recommended that an anamnesis and a clinical examination is carried out (21). It is then recommended to supplement with diagnostic imaging, blood tests and biopsies (21). The examinations must be of such a scope that it provides answers to histological diagnosis including subgroup with relevant histochemical markers, distribution with tumor, nodes, and metastases (TNM) and clinical stage and the patient's health/suitability for treatment (21).

According to the national action program, these clinical symptoms should lead to referral in the package course: hemoptysis (coughing up blood) and unexplained and persistent (> 3 weeks) cough, chest/shoulder pain, dyspnoea, weight loss, chest findings, hoarseness, finger-clubbing (21). Often, the investigation will start with a normal X-ray of the lungs, but a normal X-ray will never be able to rule out cancer (21). So for all practical purposes, if there is a reasonable suspicion of lung cancer,

one will proceed with a CT thorax/abdomen with intravenous contrast (21). If the CT scan shows extrathoracic disease or contralateral lung metastases (M +), the patient is unsuitable for curative treatment (with a few exceptions) (21). If CT only shows intrathoracic disease (M -), the patient is potentially eligible for curative treatment and a PET-CT should then be taken before further biopsy (21). Biopsy of the primary lesion is only relevant if there are no metastases or spread to lymph nodes (N0) (21). This means that patients with widespread disease (M+ and/or N+) are most often not available for curative treatment (21).

Once the imaging examinations have been carried out, then the biopsy can be performed. Before curative treatment can be initiated, the diagnosis should be confirmed cytologically and histologically after the radiological examination. There are various techniques to get the biopsy done. It can be done ultrasound-guided, CT-guided, through pleural puncture or with the help of endobronchial ultrasound (EBUS) (21). **Figure S3** provides a summary of the investigation with diagnostic imaging and biopsy (21).

1.3.3 Histopathology

The "rough classification" of histological subtype of lung cancer is done by looking at a paraffin-embedded and stained biopsy under a light microscope (21). Pathologists have many aids, particularly in the form of immunohistochemistry (IHC), which facilitate first-line diagnostics (21). Based on this visualization and different types of staining, the pathologist can determine which main group of lung cancer it is (21). Because medicine has become more personalized, one cannot make a treatment recommendation based solely on the histological subtype of lung cancer. Since there are several genetic variations that can have treatment consequences for the individual type of cancer, next-generation sequencing is now performed on all types of non-small cell lung cancer (see later) with the exception of squamous cell carcinoma (21).

When lung cancer is classified, it is important to distinguish between primary lung cancer (PLC) and intrapulmonary metastasis (IPM). It is important both with regard to treatment strategies, but also for prognosis (23). Unfortunately, this can be a complicated process, especially where the PLC has similar histology to IPM (23). But not only is it important to be able to distinguish between PLC and IPM, but also the

various subtypes of PLC. Lung cancer is a heterogenous disease with wide-ranging clinicopathological features (24). PLC can be classified into mainly two entities: non-small cell lung cancer (NSCLC), which accounts for 85% of the total number of diagnosis, and small cell lung cancer (SCLC), which accounts for 15% of diagnoses (24). It is therefore NSCLC that is the most common histological form of lung cancer (21, 24). Under the main types of NSCLC and SCLC, different histological subtypes are found (19, 24).

1.3.3.1 Non-small celled lung cancer (NSCLC)

Within the NSCLC classification, lung adenocarcinoma (LUAD) are the most common subtype of lung cancer, followed by squamous cell carcinoma (24). In the past, squamous cell carcinoma was the most common form of NSCLC, but has now declined, partly due to the decline in smoking in high-income countries and the composition of cigarettes (24, 25). The third most common form of NSCLC is large cell carcinoma, which accounts for around 10-15% of the subtypes (19). Other less common subtypes account for approximately 20% of all NSCLC (19). Examples of such histological subtypes are adenosquamous carcinoma, pleomorphic sarcomatoid carcinoma, large-cell neuroendocrine carcinoma, and carcinoid tumor - which alone only accounts for a few percent (19). See **Figure S4** for an overview of the various histological subtypes of NSCLC (19).

1.3.4 The TNM classification of lung cancer

When the radiological and histological response is available, a TNM stage can be set. Staging for cancer is done using TNM (21, 26). The TNM status of the patient is very important to know in order to be able to provide the correct treatment and to be able to predict the prognosis (21). It is well known that the TNM stage is closely related to the prognosis of the patient (21). See **Table S2** for an overview of the latest TNM classification for NSCLC (26).

1.4 Treatment strategies and prognosis of NSCLC

Over the past few years, mortality from NSCLC has decreased significantly, mainly due to earlier diagnosis, but also because new therapeutic strategies have been developed (21). For the first time in history the 5-year survival rate for all types of lung cancer was a total of 30.0% in Norway in 2022, where the median survival have increased from 9.2 months in 2011 to 16.8 months in 2022 (3). It is difficult to

calculate an exact 5-year survival for NSCLC as there are many subgroups, but the 5-year survival was 38.3% for adenocarcinoma and 31.6% for squamous cell carcinoma in 2022 (3). In comparison the 5-year survival rate for SCLC was only 8.6% in 2022 (3). In any case, it is important to be aware that the survival rate depends on several factors, including which histological subtype the patient has or, not least, which TNM stage the cancer is in at the time of diagnosis. In patients with localized NSCLC, i.e. the cancer has not spread outside the lungs at the time of diagnosis, the 5-year survival rate is 63% (27). For regional NSCLC, which means that cancer has spread outside the lungs to regional lymph nodes, the 5-year survival rate is 35% (27). For metastatic NSCLC, the 5-year survival rate is only 7% (27).

Both surgery and radiation therapy are treatment modalities that can provide curation in patients with stage I-III NSCLC (21). Primarily, surgery is to be recommended for patients in early stages who are medically and technically operable (21). In patients who are inoperable or who do not want surgery, radiation therapy is an alternative (21). Chemotherapy alone is not curative, but together with surgery and/or radiotherapy can increase the possibility of a cure (21). For stage I, surgery alone is recommended, while in stage II, surgery is combined with adjuvant chemotherapy in patients under 70 years of age (21). Stage III is a heterogeneous group where optimal treatment is differentiated in relation to T- and N-stage. Patients with stage IV disease are usually not available for curative treatment (21).

Regardless of whether the patient is intended for curative treatment or not, the patient will often receive some sort of chemotherapy and/or immunotherapy (21). Traditionally, platinum-containing chemotherapy is used in the treatment of NSCLC and is considered the cornerstone of chemotherapy for lung cancer (21). Over the past few decades, it has also become more and more common to test lung cancer for genetic mutations. There is now immunotherapy that attacks cancer-driven activating mutations in lung cancer cells (21).

1.5 Genetic mutations in lung cancer

As mentioned, there are several genetic mutations which are considered risk factors for developing lung cancer (28). Over the years, a number of drugs have been developed to target these genetic mutations, and today there are many targetable genes in NSCLC (21). The most important genetic mutations for which targeted

treatment is currently available for based on their prevalence, are KRAS (Kirsten rat sarcoma viral oncogene homologue), EGFR (epidermal growth factor receptor), ALK (anaplastic lymphoma kinase), BRAF (v-raf murine sarcoma viral oncogene homolog B1), ROS1 (Proto-Oncogene 1, Receptor Tyrosine Kinase), NTRK (Neurotrophic Tyrosine Receptor Kinaseand) MET (Mesenchymal Epithelial Transition) (21, 28). See **Figure S5** for a complete overview of the incidence of the various oncogenes in NSCLC (28).

KRAS is the most common oncogene in lung cancer, with 30-38% NSCLC cases harboring the mutation (28). The gene controls proteins involved in cell growth, maturation, and death. Activating mutations cause uncontrolled growth and maturation (29). Sotorasib is the only approved drug targeting the KRAS G12C mutation in Norway, prolonging overall survival by 12.5 months. EGFR mutations are the second most common in NSCLC, found in 10-15% of cases (21). Mutations lead to constant activation of the EGFR signaling pathway, resulting in malignancy. Although EGFR mutations are less common, several approved drugs like gefitinib, erlotinib, afatinib, dacomitinib, and osimertinib treat advanced EGFR-mutated NSCLC (21).

Figure S5 shows that KRAS and EGFR account for the majority of mutations in NSCLC, where the other associated mutations alone only account for a few percent (28). Despite this, they collectively make up about a quarter of the oncogenes (28). What the aforementioned mutations have in common is that there are a number of targetable therapies against them and more are under development (21). For example, there are a number of approved drugs for both ALK, BRAF, ROS1, NTRK and MET mutations (21).

1.6 T cell-inflamed vs. non-T cell-inflamed NSCLC

Immunotherapy such as checkpoint blocking antibodies and adoptive cell transfer is becoming more and more commonly used for many types of cancer, and lung cancer is no exception (30-32). Although immunotherapies can be effective, many people fail to respond and some develop resistance (30). It is known that especially the tumors with high expression of dendritic cells and CD8 T cells - so-called “T-cell inflamed" or “hot” phenotypes, respond well to immunotherapy and generally develop less resistance (30, 33, 34). Conversely, one can also say that tumors that have a low

expression of these cell types - "non-inflamed" or “cold” phenotypes, will preferentially have a poorer response to immunotherapy and more often develop resistance (30, 34). In that way, the inflammation signature can be used to help predict the immunotherapy response (30, 34).

Galon et al. proposed different methods for immune phenotyping of tumor tissue to better understand and treat various tumor immune profiles (35). Tumors can be classified as immune hot, altered/excluded, or cold based on their immune cell infiltration and activation, see **Figure S6** (34, 35). Immune hot tumors have a high immune cell infiltration, while altered tumors exhibit partial infiltration, and cold tumors show minimal or no infiltration (35). These classifications have implications for the effectiveness of immunotherapies and can be used guide personalized treatment strategies (35). Immune phenotyping involves the assessment of immune cells, their spatial distribution, and functional state in the tumor microenvironment (35). Several methods are employed for this purpose, including IHC and gene expression profiling (35).

Because it has been seen that immunological parameters provide prognostic information for the outcome of lung cancer, research is being done to develop a TNM-I score as a supplement to the already existing TNM score (31, 32). The advantage of such a TNM-I score is that you can get even more personalized medicine and to a greater extent be able to determine which patients will be able to benefit from immunotherapy (32). Today, little is known about which patients who will benefit from immunotherapy, and the objective response to immunotherapy in NSCLC patients is around 20%. Therefore, there is an urgent need to be able to predict survival and response to immunotherapy in this patient group (32, 36).

1.7 Genetic mutations associated with a low T cell-signature

As mentioned, research up to date has concluded that most forms of NSCLC are driven by defects in the genes mentioned in section 1.5 (21, 28, 29, 37-39). But in addition to these genes, defects have also been found in other genes that have been shown to induce cancer (37).

1.7.1 STK11

STK11 is a gene encoding for liver kinase B1 (Lkb1), which plays an important role in metabolism, cell polarity and DNA repair (40-44). STK11 is found on chromosome 19 and consists of nine coding exons and one non-coding exon (40, 43, 45). The Lkb1 protein is expressed in all forms of tissue throughout the body. In order for the Lkb1 protein to carry out genetic regulation, it must be activated (40). Like many other proteins, its activation is post-translationally modified by phosphorylation, acetylation and ubiquitination (40, 46). When Lkb1 proteins are active, it in turn activates a number of proteins in the AMP-activated protein kinase (AMPK) family (40, 47). The physiological role of Lkb1 is to modulate the metabolism of the cell in response to low nutrition and other stressors (40). When the Lkb1 protein is transcribed, it leads to a down-regulation of anabolic pathways and up-regulation of catabolic processes, see **Figure 1** (40, 45, 47). This effect is mediated by Lkb1 through the AMPK signaling pathway. Loss of Lkb1 activity leads to a metabolic shift in the cell from oxidative phosphorylation to increased aerobic glycolysis and glutamine catabolism. This shift is a hallmark of malignant cells (40, 45, 48). A pathway that is closely regulated by Lkb1 and AMPK, with major consequences for tumorigenesis, is the mammalian target of rapamycin (mTOR) signaling pathway (40, 46). Activated AMPK phosphorylates mTOR and leads to the translation of key proteins involved in cellular proliferation and advancement through the cell cycle (40, 41). With loss of Lkb1 function, these proliferation pathways will be constantly upregulated. Therefore, it can be said that the Lkb1 protein and thus the STK11 gene acts as a tumor suppressor (45).

Mutations in the STK11/LKB1 gene have been recognized as an important tumor suppressor since the 90s (37, 45). While STK11/LKB1 mutations are commonly detected in lung adenocarcinomas, they are also present in pulmonary squamous cell carcinoma and large cell adenocarcinoma (40, 49-51). These mutations frequently coincide with KRAS mutations and are believed to contribute to the formation of aggressive tumors with metastatic properties, leading to a reduced overall survival rate (41, 51). It has been demonstrated that STK11 mutations have been shown to correlate with a smoking-associated molecular signature, which in turn means that STK11 inactivation increases the chance of tobacco-induced carcinogenesis (40, 52).

In addition to an association between STK11-mutation and the AMPK/mTOR signaling pathway, a connection between STK11 expression and the stimulator of interferon genes (STING) pathway has also recently been discovered (44, 53). STING is a protein found in the cytoplasm that is activated by the presence of free double-stranded DNA (dsDNA) in the cytoplasm. It is thus the presence of pathogenic microbes or neoplastic transformation that can lead to the activation of STING (54). STING then leads to the recruitment and activation of tank-binding kinase 1 (TBK1), which in turn activates the transcription factor IRF3 to induce the production of type 1 interferon and other chemokines, which then leads to T-cell recruitment (44, 53). Kitajima et al. have therefore seen that down regulation of STING - as a result of mutations in the STK11 gene, leads to loss of chemokines that promote T-cell recruitment and can thus be said to drive tumor escape (44, 53). Tumor cells with genetic abnormalities in the STK11 signal axis are therefore more often associated with a low T cell-signature and can therefore be said to be immunologically cold (37, 44, 55, 56).

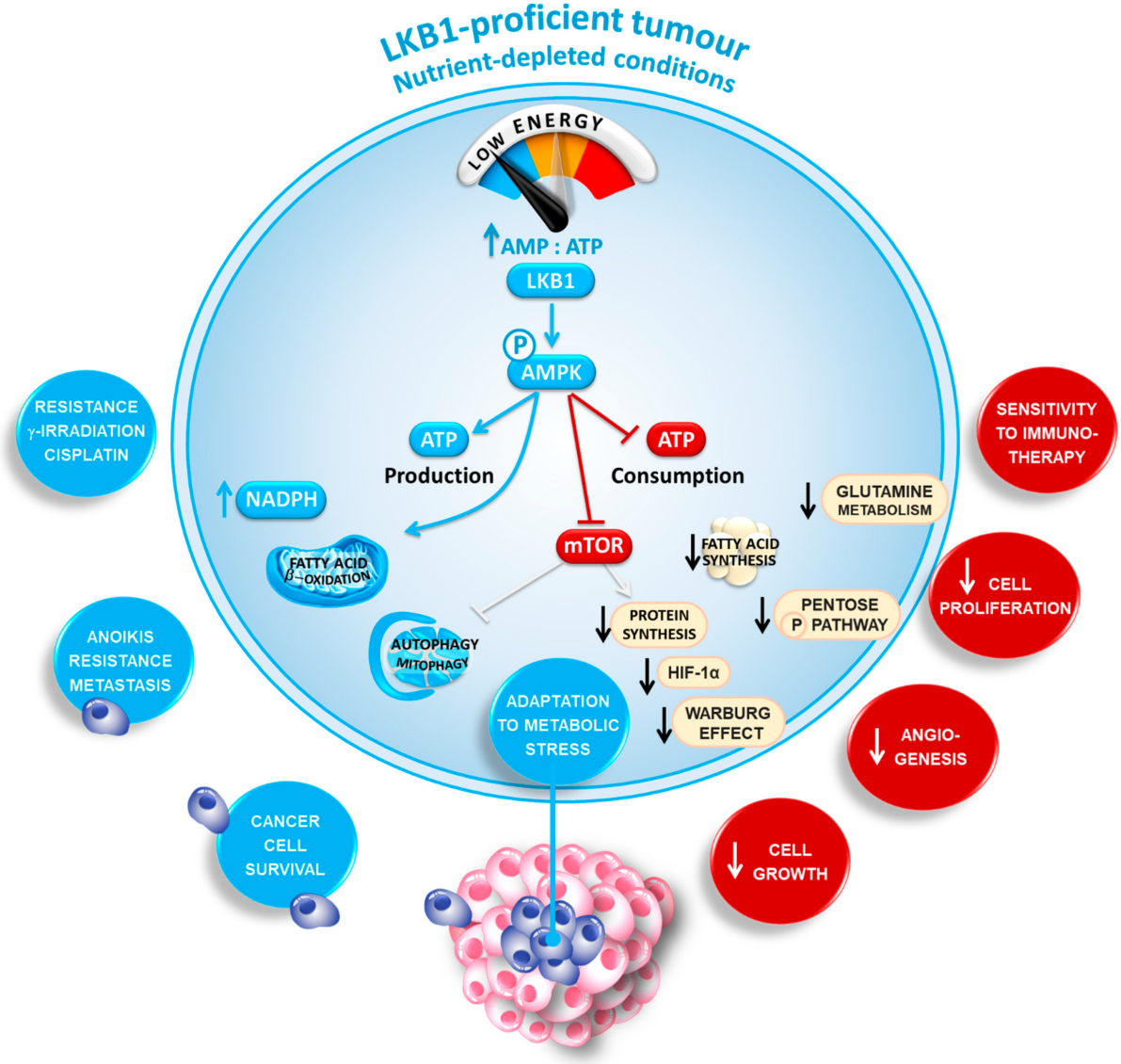

Figure 1: *LKB1 is a master metabolic sensor that acts as an energy gauge to sustain cancer cell survival (44). The figure is used with permission from the author.*

Furthermore, STK11 mutation has been associated with very poor prognosis in NSCLC (37, 40, 44, 57, 58). A possible explanation for this is that tumors with STK11 mutation responds less and more often develop resistance to PD-L1 inhibitors and other forms of immunotherapy compared to lung cancer without this mutation (37, 59, 60). One of the explanations for this is that it is seen that the STK11 gene has a central role in the expression of PD-L1 (37, 44). This connection is seen via STING, where a down-regulation leads to impaired dsDNA sensing and thus reduced expression of immune checkpoint regulatory proteins such as PD-L1 ,see **Figure 2** (44)

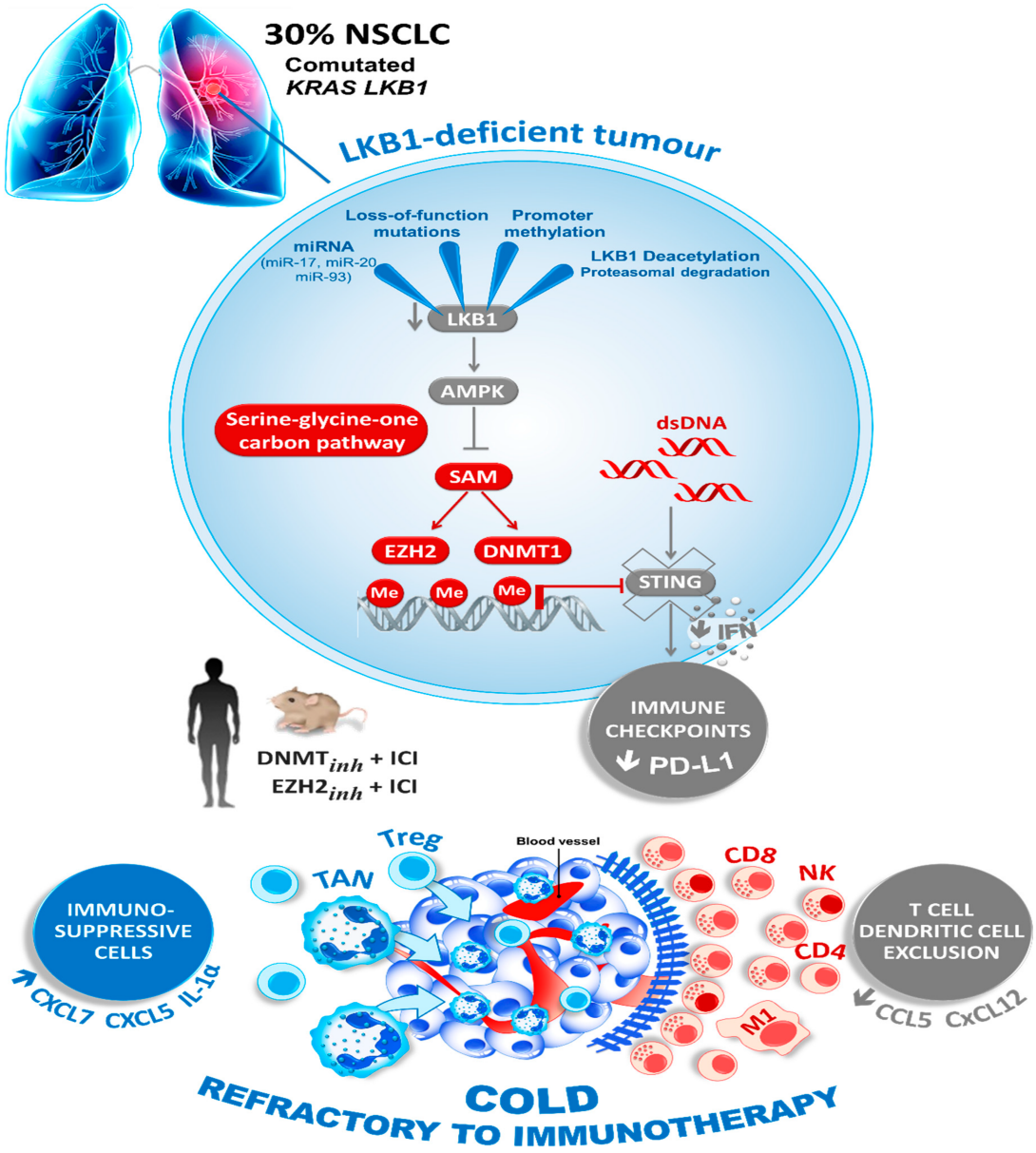

Figure 2: *Loss of LKB1 drives the tumor immune escape (44). The figure is used with permission from the author.*

1.7.2 KEAP1

Another gene where mutations have been shown to induce cancer is the KEAP1 (kelch-like ECH-associated protein 1) gene. Mutations in the KEAP1 pathway have been identified in 20-30% of all lung adenocarcinomas, making it a potentially important gene in the oncogenesis of lung cancer (61-63). The lungs represent an environment with high oxidative stress, which is tolerated through tightly regulated stress response pathways (61). A critical stress response mediator is the transcription of nuclear factor erythroid-2-related factor 2 (NFE2L2/NRF2), which is negatively regulated by the KEAP1 (61, 63).

NRF2 is part of critical stress response mediators in mammalian cells (63). Normally under hemostatic conditions in the cell with low stress, KEAP1 degrades NRF2 by binding to it together with proteosomes (61). If, on the other hand, there is a lot of oxidative stress and non-haemostatic conditions, it will lead to conformational changes in KEAP1, which in turn causes the degradation of NRF2 to stop and thus cause NRF2 to accumulate and translocate to the nucleus (61). When NRF2 nuclear translocates, it leads to the transcription of cytoprotective genes that code for detoxifying enzymes and antioxidant proteins, such as NADH (61). The induction of these genes leads to resistance to oxidative stress (61, 64). Based on this, one would have thought that having a high level of NRF2 was protective against cancer. But lung cancer with a high level of NRF2 is highly resistant to chemotherapy and radiotherapy, in addition to being aggressively proliferative in nature (65, 66). Mutations in the KEAP1 gene thus have a very poor prognosis (67, 68). How NRF2 promotes cell proliferation is not well understood, but an upregulation of NRF2 is seen when proliferative signaling pathways, such as active phosphatidylinositol 3-kinase (PI3K), are activated. When P13K is activated, it can be seen that NRF2 augments the expression of metabolic genes that assist in driving proliferative programs (61, 64).

There is data to suggest that the activation of the Keap1-Nrf2 pathway is associated with the emergence of resistance to chemotherapy (69). In the same way as mutations in STK11, mutations in the KEAP1 gene are also associated with a lack of T-cell infiltration, and tumors that have this mutation are generally immunologically cold and therefore responds and therefore respond poorly to immune checkpoint inhibitors (ICIs) (70, 71). Over the past few years, pharmaceutical companies have directed their attention towards targets in both the Keap1-Nrf2 and the STK11-AMPK pathway to discover new and efficient molecules that can hinder the interaction these pathways have (69). A notable benefit of targeting these molecules is the anticipated enhancement in the effectiveness of conventional antitumor chemotherapies, and then especially for ICIs (69).

2 The aim of this thesis

The presence of mutations in the STK11 gene, frequently accompanied by mutations in the KEAP1 gene, has been associated with poor outcomes in NSCLC patients undergoing immunotherapy (55). However, the underlying biology remains unknown.

Our research has revealed that patients who harbor co-mutations in STK11 and KEAP1 genes predominantly exhibit a cold immune phenotype (72). The main aim is to explore whether the co-mutations or individual alterations in STK11 and KEAP1 genes are the key drivers of poor local immune infiltration and potential resistance mechanisms to immunotherapy in NSCLC.

By studying the underlying mechanisms that govern the immune microenvironment in NSCLC, we hope to shed light on the specific factors that lead to the development of a cold immune phenotype. Ultimately, our findings may help to inform the development of new treatment strategies for NSCLC patients with STK11 and KEAP1 mutations. There are currently no effective treatments for lung cancer cases with these mutations (73).

3 Material and method

3.1 Study design

Genomic profiling was carried out on 215 patients participating in the TNM-I clinical trial (NCT03299478), with 137 of them diagnosed with lung adenocarcinoma (LUAD). Within this group, patients with STK11 and KEAP1 mutations were chosen for further investigation (n=23). The selection process for identifying variants involved excluding the following: non-exonic untranslated regions, synonymous and common polymorphisms (with a minor allele frequency greater than 1% as per the 1000 Genomes Project and GnomAD), and any variants classified as benign or likely benign in the ClinVar database (74, 75).

3.2 NanoString gene expression panel analysis

Gene expression analysis was performed using the NanoString nCounter gene expression assay. The nCounter Advanced Analysis protocol is based on direct digital detection of messenger RNA (mRNA) molecules of interest using target-specific, color-coded probe pairs (76). A pair of reporter and capture probes with target-specific sequences ranging from 35 to 50 bases are utilized to detect each gene of interest (76). The reporter probe has a unique color code at its 5' end, which acts as a molecular barcode for the genes of interest, whereas the capture probes have a biotin label at their 3' end, facilitating the attachment of target genes for downstream digital detection (76).

Following hybridization of the target mRNA with the reporter-capture probe pairs in solution phase, excess probes are eliminated, and the probe/target complexes are aligned and immobilized within the nCounter cartridge (76). The cartridge is then placed in a digital analyzer for image acquisition and data processing (76). The surface of the cartridge displays hundreds of thousands of color codes indicating mRNA targets of interest (76). The expression level of a gene is measured by counting the frequency of the corresponding color-coded barcode detected, and the barcode counts are then tabulated (76). See **Figure S7** for a graphical representation of the workflow of the nCounter analysis (77)

3.2.1 nCounter PanCancer IO 360™ Panel

In this project, more specifically, the gene panel nCounter PanCancer IO 360™ was used to analyze the background genes relevant to the project. The panel comprises

of 770 clinically relevant genes and signatures associated with immune-targeted and other therapies (77).

Once the samples with single STK11 mutation, single KEAP1 mutation and co-mutation had been identified, these were marked and transferred to an Excel document with an overview of their mutation status. The samples' corresponding genetic data were then labeled in the same way as in Excel and compressed into RCC files.

3.3 Rosalind and nCounter analysis

After the NanoString gene expression panel samples were completed, the RCC-files with the expression data was uploaded and analyzed by ROSALIND®. ROSALIND is a cloud-based software platform that enables analyzation and interpretation of different gene expression data (78).

3.3.1 Quality control metrics and normalization

Before the actual analysis is carried out, ROSALIND starts by providing multiple metrics to verify the quality of the data (79). Any issues detected in the samples will be automatically flagged and the issue detected will be displayed for easy interpretation of the quality control (QC) metrics (79). For nCounter experiments, the following QC metrics are performed: imaging quality - the percentage of fields of view (FOV) captured (0.75% or lower causes flag), binding density - concentration of barcodes seen by the instrument (<0.1 or > 2.25 causes flag), in spots per square micron, and control linearity - a correlation analysis in log2 space between the known concentrations of positive control target molecules added by NanoString and the resulting counts (< 0.95 causes flag) (79). In addition, ROSALIND performs QC with regard to the noise threshold, i.e. the limit of detection of the assay (minimum expression level detectable) by calculating how many standard deviations the 0.5fM Positive Control value is above the average Negative Control value (QC flag occurs if below 2) (79). Limit of detection QC reports the average Negative Control value (“Mean”), standard deviations of Negative Controls (“Std Dev”) and 0.5fm Positive Control value (“Pos Control E”) - where QC flag occurs if “Mean” + 2 * “Std Dev” is greater than “Pos Control E” (79). All the samples passed the built-in QC metrics, including FOV, binding density, control linearity, mean of negative controls (Mean),

standard deviation of negative control (Std Dev) and positive control (Pos Control E). Se **Table S3**.

Another important step before the actual processing of the data can start in ROSALIND, is to perform data normalization. Data normalization ensures the validity of its downstream analyzes (80). ROSALIND follows the NanoString nCounter® Advanced Analysis protocol for data normalization of Gene Expression nCounter RCC Analysis, where the normalization is performed by dividing counts within a lane by the geometric mean of the normalizer probes from the same lane (81). Normalizer probes are selected by the geNorm algorithm as implemented in the Bioconductor package NormqPCR R library (81, 82).

Differential gene expression analysis was performed utilizing volcano plots. Fold changes (FC) and adjusted p-values were calculated using criteria provided by Nanostring (-1.5<FC>1.5; adjusted p-values <0.05). Clustering of genes for the final heatmap of differentially expressed genes was done using the partitioning around medoids method using the fpc R library that takes into consideration the direction and type of all signals on a pathway, the position, role and type of every gene (78, 83). By comparing the expression data from different experimental conditions or groups, these plots highlight genes with substantial FC and statistical significance.

3.3.2 Pathway analysis

Another way to explore gene expression is through gene expression signatures (GES), which is a single or combined group of genes in a cell with a uniquely characteristic pattern of gene expression that occurs as a result of an altered or unaltered biological process or pathogenic medical condition (84-86). GES are commonly defined as “a ranked list of genes whose differential expression is associated with a particular biological phenomenon” (87-89).

3.3.3 Nanostring pipeline

Based on the GES, a gene set analysis (GSA) score is calculated, which provides an average of the significance measured across all the genes in the pathway, as calculated by the differential expression (90). The global significance score (GSS) assess the overall significance of changes within a pathway and are always positive, regardless of whether the genes are up- or down-regulated (90). On the other hand,

directed GSS (dGSS) gives a negative or positive value corresponding to down-regulation or up-regulation of a pathway (90). These scores are scaled to the same distribution (t-statistic), which makes them more robust for comparisons across different pathways or experiments (90). A high score indicates that a large proportion of the genes in a pathway are exhibiting changes in expression across groups of samples (90).

3.3.4 Other analytical approaches

Gene Set Enrichment Analysis (GSEA) is a statistical technique employed to identify groups of genes or proteins that are significantly overrepresented within a large set of genes or proteins, potentially linking them to disease phenotypes (91, 92). A range of database sources were consulted for GSEA, including Interpro (93), NCBI (94), MSigDB (92, 95), REACTOME (96), WikiPathways (97, 98). However, not all of these databases were ultimately used in this thesis.

3.4 Ethical aspects and approval of the project

Ethical approval for the entire clinical trial (NCT03299478) was granted by the Regional Committee (REK) and the Norwegian Data Protection Organization, under the Institutional Review Board (IRB) number REK2016/2054.

4 Results

4.1 Patient characteristics

The tissue samples included in the study came from 23 people who all had LUAD (n = 23), where the majority were in an early stage corresponding to pTNM1 (n = 14, 61%). The patients had a median age of 69 years (range 57-83), a female representation of 61% of the cohort, and at the time of diagnosis approximately half were still smokers (n = 12, 52%), while the other half had a previous history of smoking (n = 11, 48%). Thus, all the patients in the cohort had a positive smoking history. Regarding the mutation status, 43% (n = 10) of the cohort were co-mutated, while 35% (n = 35) had a single mutation with KEAP1 and 22% (n = 5) a single mutation with STK11. See **table 1.**

Clinical characteristics	n (%)	Tumor characteristics	n (%)
Age at diagnosis		**Immune phenotype based on TNMI-score**	
Median (range)	70 (57-83)	Excluded	14 (61)
Sex		Desert	9 (39)
Women	14 (61)	**pTNM stage**	
Men	9 (39)	1	14 (61)
Smoking History Category		2	4 (17)
Current	12 (52)	3a	5 (22)
Previous	11 (48)	**Mutation status**	
Surgical procedure		Co-mutation	10 (43)
Lobectomy	21 (91)	KEAP1	8 (35)
Pulmonectomy	2 (9)	STK11	5 (22)
Performance status		**Histology subtype**	
0	18 (78)	Acinar	7 (31)
1	5 (22)	Solid	9 (39)
		Papillary	5 (22)
		Lepidic	1 (4)
		Other	1 (4)

Table 1: *Patient characteristics and tumor characteristics of the population. The population contains no people with a negative smoking history, as well as no patients with a TNM stage higher than 3a, as these are inoperable. The table was created using PowerPoint.*

4.2 STK11 vs. co-mutation

The immune gene expression profiles were assessed using a NanoString panel (IO360) comprising 770 immune- specific genes and 39 signatures. Heatmap and hierarchical clustering of all genes and signatures for a combined group with single mutations vs co-mutation are presented in **Figure 3**.

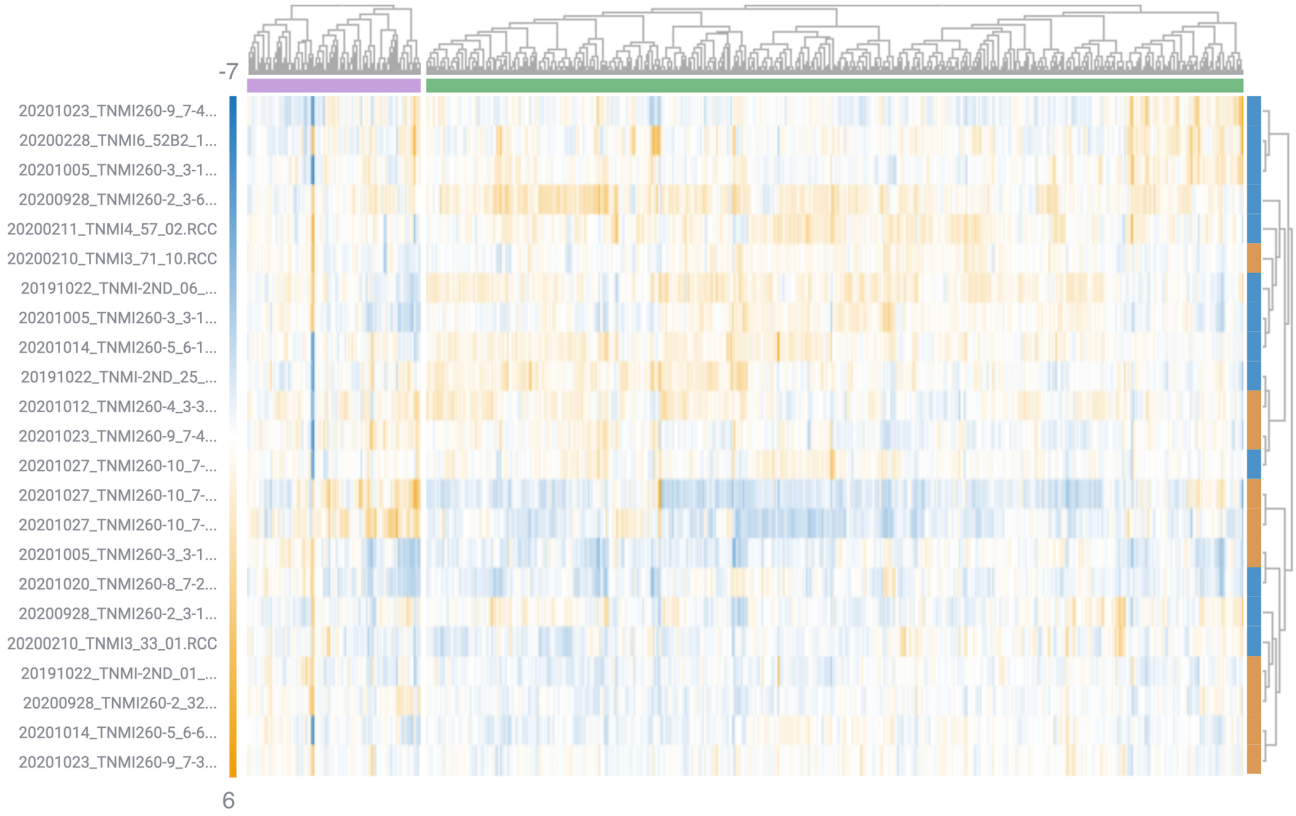

Figure 3: *Heatmaps with hierarchical clustering of all genes and signatures for the comparison between the single mutations and the co-mutations. The orange color corresponds to how positive the FC-value is, while the blue color corresponds to how negative the FC-value is. To create the heatmap, a filter with FDR-adjusted p-value < 0.99 and -1.001 ≤ FC ≥ 1.001 has been used.*

We first examined whether STK11 single mutations and STK11/KEAP1 co-mutations had different immune gene expression profiles. In the volcano plot – where STK11 is the control group and co-mutation is the baseline, there is a significant number of upregulated genes in STK11 compared with co-mutation. Based on a filter where the FDR-adjusted p-value is = 0.05 and -1.5 ≤ FC ≥ 1.5, there are 120 up-regulated genes and 10 down-regulated genes (**Figure 4A)**. When the upregulated genes are sorted according to FC, FCAR (7.92), MMP9 (5.52), ITGB3 (5.14), CD79B (5.10) and CDH2 (4.59) are the genes which are most up-regulated according to FC in the STK11 samples compared to co-mutations. For down regulation according to FC, IF6 (-5.42), SLC7A5 (-4.64), CDC20 (-2.62), TGFBR1 (-2.56) and RRM2 (-2.55) have the

highest negative FC. The significantly upregulated and downregulated genes have then been analyzed and sorted by dGSS against the Nanostring Annotation GES, where **Figure 4B** shows that the “Lymphoid Compartment” (dGSS = 1.8828), “Matrix Remodeling and Metastasis” (dGSS = 1.8532), “Immune Cell Adhesion and Migration” (dGSS = 1.839), “Costimulatory Signaling” (dGSS = 1.7901) and “Cytokine and Chemokine Signaling” (dGSS = 1.7689) are the GES with the highest dGSS.

This was further confirmed using enrichment analysis via PanglaoDB Database, where genes associated with adaptive immunity were up-regulated. More specifically, we found that that B cells are generally upregulated (p-adj = 0.01489), and memory B-cells (p-adj = 0.11801) (**Table S4**).

The up-regulation of the immune system and especially the up-regulation of B cells, is confirmed by the GSEA pathway analysis (GO data set), where go_cell_activation (p-adj = 0.00074) and go_b_cell_activation (p-adj=0.03088) is statistically significant, in addition to go_lymphocyte_activation also tends towards being statistically significant (p-adj = 0.05447) (**Table S5)**.

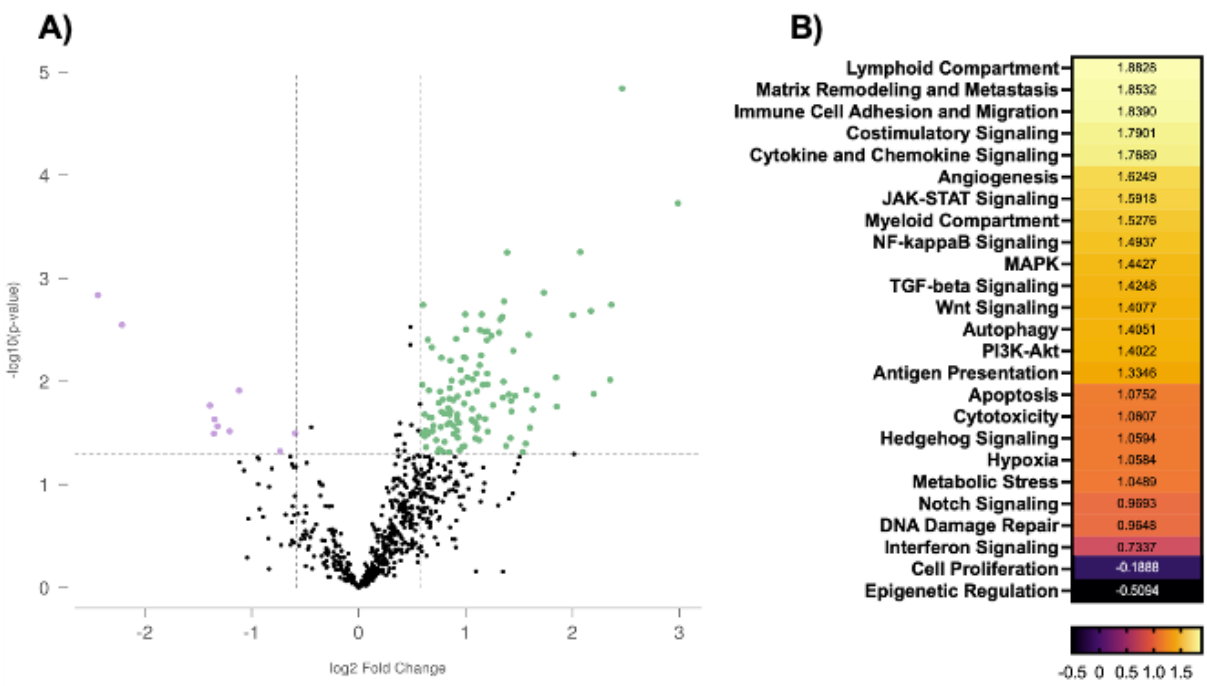

Figure 4: *Overview of the genetic data. (A) Volcano plot showing the difference in up- and down-regulated genes in the STK11 samples compared to the co-mutation samples.The green dots represent up-regulated genes in the STK11 samples, while the purple dots represent the down-regulated genes. (B) dGSS for the various Nansotring Annotations pathways, where a lighter color represents a more positive dGSS and a darker color more negative dGSS. The tables are sorted from the largest positive value at the top to the most negative value at the bottom. The figures are generated by ROSALIND®, Prism 9® and PowerPoint.*

4.3 KEAP1 vs. co-mutation

In the volcano plot – where KEAP1 is the control group and co-mutation is the baseline, there are five significantly up-regulated genes and no down-regulated genes compared to the control group. The five significantly up-regulated genes with the filter FDR-adjusted p-value is = 0.05 and FC is -1.5 ≤/≥ 1.5 in the volcano plot by decreasing FC, are MMP7 (5.19), WNT5A (4.68), ITGB8 (4.58) MMP9 (3.34) and SGK1 (2.23) (**Figure 5A**)**.**

Pathway analysis revealed that Immune Cell Adhesion and Migration (dGSS = 2.0167), “Matrix Remodeling and Metastasis” (dGSS = 1.9569), “Myeloid Compartment” (dGSS = 1.9449), “Wnt Signaling” (dGSS = 1.9244) and “Hedgehog Signaling” (dGSS=1.8115) sigantures are the pathways with the highest dGSS. **Figure 5B** shows that “Lymphoid compartment” (dGSS = 1.4241) is ranked lower in KEAP1 compared to STK11.

Consistently, there were very many pathways in the GSEA (reactome database) which were statistically significantly upregulated. **Table S6** shows that both “ activation of matrix metalloproteinases” (p-adj = 0.00695), “ degradation of the extracellular matrix” (p-adj = 0.03771), “ extracellular matrix organization” (p-adj = 0.03771), “reactome collagen formation” (p-adj = 0.03771), “ collagen degradation” (padj = 0.03771), “ assembly of collagen fibrils and other multimeric structures” (p-adj = 0.03771) and “ extracellular signal” (P-adj = 0.03771) were statistically significantly upregulated. The genes matrix metalloproteinase (MMP) 7 and MMP9 – which are part of these pathways, were the two genes with the highest FC (5.19, 3.34). In addition, the three genes WNT5A, ITGB8 and SGK1 were statistically significantly upregulated in the MSigDB oncogenic signatures pathway with a p-adj = 0.03417.

An almost significant up-regulation of the TSUNODA_CISPLATIN_RESISTANCE_DN pathway was also found by GSEA (MSigDB - Chemical and Genetic Perturbations). The two genes WNT5A and SKG1 were significantly increased in single KEAP1 mutation compared to co-mutation, where respectively WNT5A had an FC of 2.22504 (p-value < 0.05) and SKG1 1.15948 (p-value < 0.05) (**Table S7)**.

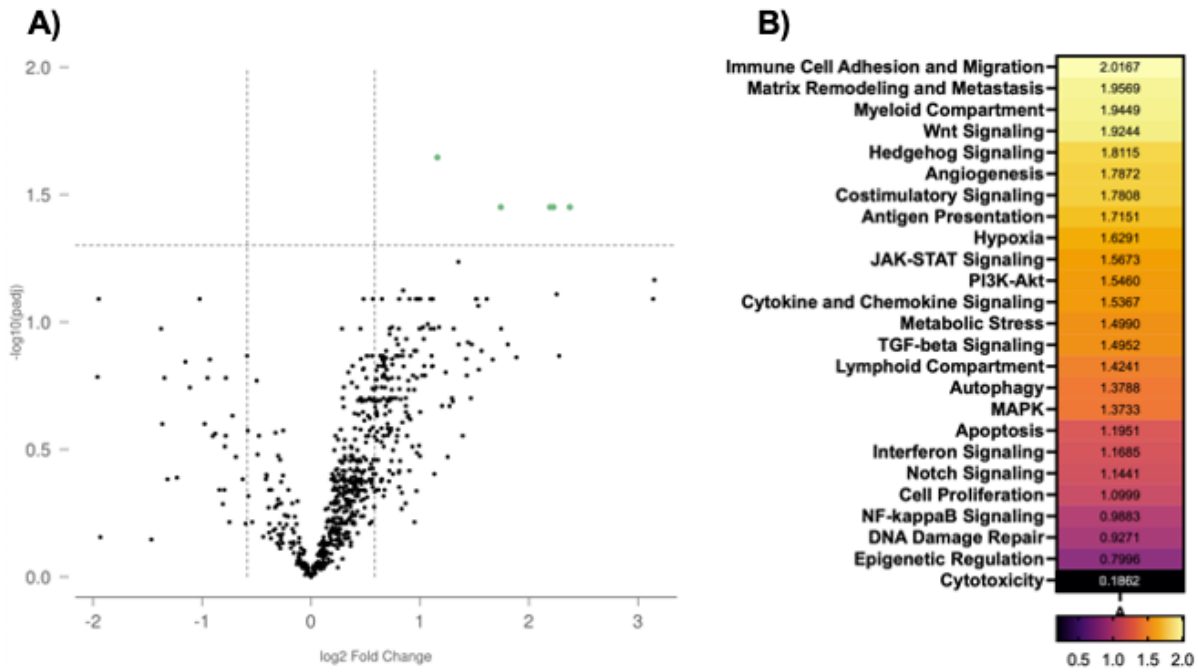

Figure 5: Overview of the genetic data. (A) Volcano plot showing the difference in up- and down-regulated genes in the STK11 samples compared to the co-mutation samples. The green dots represent upregulated genes in the KEAP1 samples. (B) dGSS for the various Nansotring Annotations pathways, where a lighter color represents a more positive dGSS and a darker color more negative dGSS. The tables are sorted from the largest positive value at the top to the most negative value at the bottom. The figures are generated by ROSALIND®, Prism 9® and PowerPoint.

4.4 STK11 vs. KEAP1

In the volcano plot – where KEAP1 is the control group and co-mutation is the baseline, with the filter FDR-adjusted p-value is = 0.05 and FC is -1.5 ≤/≥ 1.5 18 significantly up-regulated genes and 14 significantly down-regulated genes (**Figure 6A**). The nonstring pathway analysis shows that dGSS is highest for “NF-kappaB Signalling” (dGSS = 0.9034), “lymphoid compartment” (dGSS = 0.8864) and “cytotoxicity” (dGSS = 0.7454). dGSS is lowest for “Myeloid compartment” (dGSS = -0.8049) “Wnt Signalling” (dGSS= -0.88724), “Cell proliferation” (dGSS= - 0.9524) and “Hedgehog Signalling” (dGSS= - 0.9875) (**Figure 6B)**.

Although it is not statistically significant, the trend in the PangloaDB cell types database is that B-cells and its subtypes are upregulated in STK11 compared to KEAP1, but none of the adjusted p-values are under threshold and the different adjusted p-values for other cell types is quite similar (**Table S8**). The same trend is also observed when analyzing against the Panther library where “B cell activation”

has a (p-adj = 0.18602), where the B-cell genes CD79B, CD79A, PIK3CD and IKBKB are up-regulated in the STK11 compared to KEAP1 (**Table S9**).

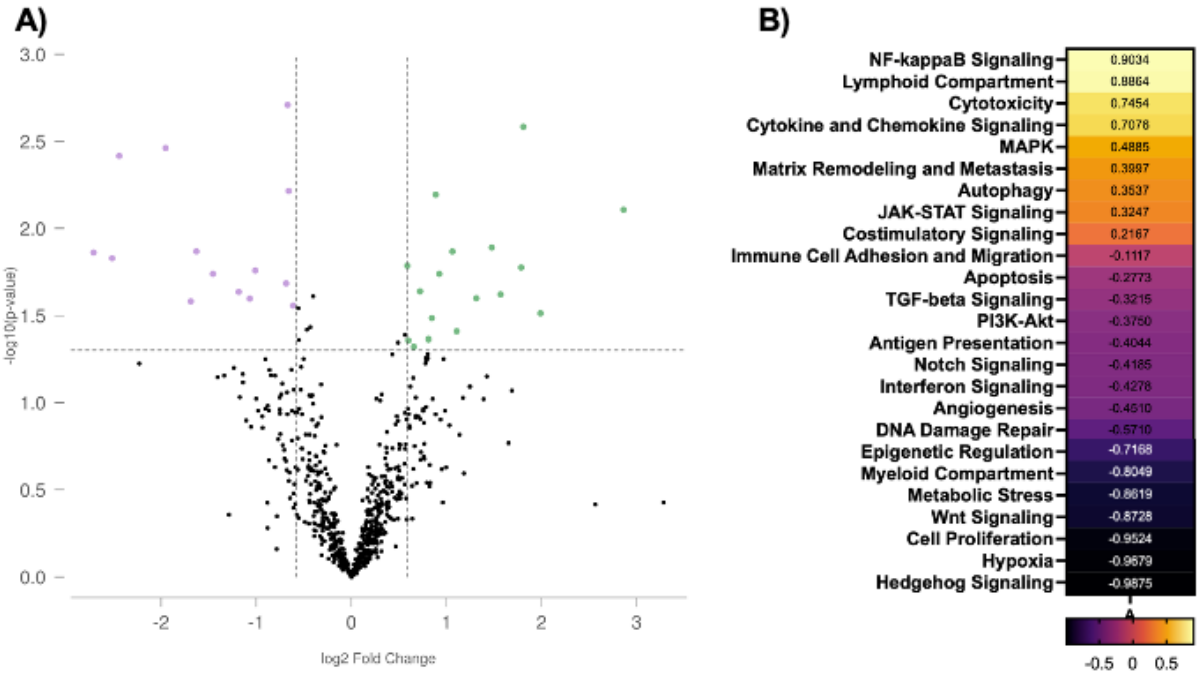

Figure 6: *Overview of the genetic data. (A) Volcano plot showing the difference in up- and down-regulated genes in the STK11 samples compared to the co-mutation samples. The green dots represent up-regulated genes in the STK11 samples, while the purple dots represent down-regulated genes. (B) dGSS for the various Nansotring Annotations pathways, where a lighter color represents a more positive dGSS and a darker color more negative dGSS. The tables are sorted from the largest positive value at the top to the most negative value at the bottom. The figures are generated by ROSALIND®, Prism 9® and PowerPoint.*

5 Discussion

In this master thesis, we investigated the potential drivers of the non-inflamed phenotype observed in early stage (stage I-IIIA) lung adenocarcinoma patients with KEAP1 and STK11 mutations. Our findings suggest that KEAP1 mutation plays a more significant role in the development of the immune desert phenotype compared to STK11 mutation. In addition, our results indicate a possible association between KEAP1 mutation and chemoresistance in these patients. This study contributes valuable insights into the molecular mechanisms underlying the poor response to immunotherapy observed in NSCLC patients harboring KEAP1 and STK11 alterations. Understanding these mechanisms may facilitate the development of novel therapeutic strategies for patients with these mutations, ultimately improving their prognosis and treatment outcomes.

In this context, Papillon-Cavanagh et al. investigated the predictive versus prognostic effect of STK11 or KEAP1 mutations in non-squamous NSCLC, where they included a group with co-occurring STK11, KEAP1 and KRAS mutations (99). They found that mutations in STK11-KEAP1 serve as prognostic biomarkers rather than predictive ones for the efficacy of immune check points blockers (99). Shen et al. found in their study that co-mutation with both STK11 and KEAP1 to be a strong determinant for an unfavorable prognosis with currently available therapies, where the median overall survival for the patients with co-mutations of STK11/KEAP1 in KRAS mutation-positive lung cancer was just 7.3 months (100).

5.1 KEAP1 mutation induces an upregulation of oncogenic and metastatic pathways

The most obvious finding in the study is that STK11 has a very high number (n = 120) of upregulated genes compared to the co-mutation group. The up-regulated genes in Nanostring GSA for the STK11 vs co-mutation comparison are involved in pathways that represent immunological response and activation of the immune system. It suggests that patients with a single STK11 mutation have a more active immune system compared to co-mutation, who appear to have a suppressed immune system. On the other hand, the KEAP1 group has a very low number of genes which are upregulated and most of the genes in the Nanostring GSA are associated with cancer pathways rather than immunological pathways (**Figure 5A/B**).

This is also confirmed in the comparison with STK11 vs KEAP1, where the same trend is observed, where the immunological pathways are up-regulated in STK11 and down-regulated in KEAP1 (**Figure 6A/B**). It suggests that the immune system alters and suppresses when the KEAP1 mutation is present, at the same time as the oncological pathways are upregulated.

It is especially the “Matrix Remodulating and Metastasis” pathway in the Nanostring GSA that is upregulated in the samples containing KEAP1 mutation, where the comparison with KEAP1 vs co-mutation has a very high dGSS (= 1.9569). STK11 vs co-mutation also has a fairly high dGSS value (= 1.8532) for the same pathway, but this pathway is even stronger for KEAP1, which supports that the progression and the disease itself is more aggressive when KEAP1 mutation is present. This observation was further confirmed by GSEA using the Reactome data set, which showed that many of the extracellular matrix pathways were statistically significant upregulated in KEAP1 samples (**Table S6**). It was especially the genes MMP7 and MMP9 that were upregulated in KEAP1. These genes are known to participate in disruption, tumor neovascularization, and subsequent metastasis of cancer (101). The mechanism for how MMPs drive oncogenesis is believed to be multimodal, where they play a role in cancer angiogenesis through their proteolytic action on proteins in the extracellular matrix (101). In addition, they also have an oncogenic effect through the release of extracellular matrix-bound proangiogenic factors such as vascular endothelial growth factor (VEGF) (101, 102).

When further analyzes of the immunological pathways which were up-regulated in the STK11 samples have been carried out, it is particularly genes of B-cell nature which are up-regulated (**Table S4**). For both the co-mutation samples and the single KEAP1 samples, no such up-regulation of immunological pathways is seen. It therefore appears that the KEAP1 mutation – both as a single mutation, but also as a co-mutation, limits the immune system and contributes to a lowered immune cell infiltration. This hypothesis is also supported by the fact that the volcano plot did not show any major genetic differences between KEAP1 vs co-mutation, where only 5 genes were up-regulated in the KEAP1 samples compared to the co-mutation (**Figure 5A**).

5.2 KEAP1 and STK11 mutation triggers a shift of immunological compartments

When investigating which pathways the upregulated genes were involved in, the “Lymphoid Compartment” was the pathway with the highest dGSS compared to the co-mutation. This is in contrast to KEAP1, where the “Myeloid Compartment” had an even higher dGSS (= 1.9449) and the lymphoid compartment a much lower dGSS (= 1.4241) compared to co-mutation. This suggests that there is a shift of compartment depending on which mutation is present. This is further supported in the comparison with STK11 and KEAP1, where the lymphoid compartment has a positive dGSS (= 0.8864) while the myeloid compartment has a negative dGSS (= -0.8049).

Myeloid-derived cells, particularly myeloid-derived suppressor cells (MDSCs) and tumor-associated macrophages (TAMs), have been identified as key players in the progression of lung cancer due to their pro-tumoral activities and negative prognostic impact (103, 104). These myeloid subsets contribute to the formation of a supportive tumor microenvironment by promoting angiogenesis, immune evasion, and tumor cell proliferation (105). These cells exert their pro-tumoral effects by suppressing anti-tumor immune responses, mainly through the inhibition of T cell proliferation and the promotion of regulatory T cells (Tregs) (106). Furthermore, MDSCs and TAMs can produce pro-inflammatory cytokines such as IL-6, IL-10, and TGF-β, which promote tumor growth and invasiveness (107). The presence of MDSCs in lung cancer tissue has been correlated with advanced stages of the disease and poor clinical outcomes (108).

Regardless, it is striking that the STK11 mutation has an up-regulation of genes involved in the lymphoid compartment, while KEAP1 has an up-regulation of genes involved in the myeloid compartment. However, further investigation is warranted into the cross-communication between MDSCs presence and KEAP1 alterations.

5.3 NF-κB pathway

In the comparison between STK11 and KEAP1, it was the Nuclear factor kappa-light-chain-enhancer of activated B cells (NF-κB) pathway in the Nanostring annotations library that had the highest dGSS score (= 0.9034) of all the pathways. The NF-κB pathway consists of five transcription factors that regulate cellular processes (109). The pathway has received much attention in the last three decades, where a large

number of human cancers have constitutive NF-κB activity due to the inflammatory microenvironment and various oncogenic mutations (109). The pathway induces the expression of various proinflammatory genes, including several genes encoding cytokines (110). The NF-κB pathways play essential roles in T-cell and B-cell activation downstream of T cell receptor and B cell receptor engagement as well as in T-cell and B-cell development (110-112). It has been shown that NF-κB activation in T cells increases the number of tumour-specific IFNγ-producing CD8+ T cells and is required for tumor elimination (113). Similarly, NF-κB activation in lung cancer cells induces T cell-mediated immune surveillance and results in tumor rejection owing to the expression of T cell-recruiting chemokines, including CCL2 (114).

We have recently reported that NF-kappa-B signaling is associated with the exclusion of cytotoxic T-cells in the immunological desert phenotype (72). The exact role of the NF-κB pathway in this setting is not entirely clear cut, but it is obvious that this pathway is more upregulated in the samples with STK11 compared to KEAP1. If the hypothesis that the presence of KEAP1 mutation limits the immune system and contributes to a lowered immune cell infiltration is true, downregulation of this NF-κB pathway is a possible explanation mechanism for this phenomenon.

5.4 The presence of KEAP1 mutation induces chemoresistance

Although the main purpose of this study was to investigate whether the co-mutations or individual alterations in STK11 and KEAP1 genes were the key drivers of poor local immune infiltration, there is an underlying theory that poor local immune infiltration makes one more resistant to chemotherapy. Some studies have looked at KEAP1 mutation and chemoresistance, where it has been shown that mutations in the KEAP1 gene gives increased susceptibility to chemoresistance (115, 116). Although it was not statistically significant with an adjusted p-value of 0.07837, in our study the two genes WNT5A and SK1 in the GSEA analysis were found to be upregulated in those with single KEAP1 mutation compared to co-mutation (**Table S7**). Upregulation of these two genes have been associated with chemoresistance, where the mechanism is assumed to be that therapeutic drugs are pumped out of the cancer cells thus preventing effective treatment (117). Thus, it may seem that in addition to KEAP1 providing an immunosuppressive effect and a “colder” tumor environment, the mutation also has an additive effect in the form of up-regulation of

genes that provide increased chemoresistance in other ways than through changes in the immune environment.

It suggests that if there is a KEAP1 mutation present, chemotherapy will potentially have minimal effect. If such a connection is demonstrated in larger studies, it could change clinical practice - which today is characterized by conventional chemotherapy being first attempted before, changed to the first-line treatment being instead immunotherapy against KEAP1.

5.5 Limitations of this study

An obvious weakness of this study was that a relatively small number of patients were included - with only 23 samples. It will require a similar study with a larger cohort to be able to verify the findings in this study. But despite the fact that there were a limiting number of samples, it must be taken into consideration that the incidence of the investigated mutations is quite low. It will require a large number of examined patients and resources in order to be able to find a sufficient number of samples. To find only these 23 patients, expensive genomic analyzes of 215 patients had to be carried out. It will therefore require enormous resources to put together a database with a large representative cohort. What is encouraging is that there is more routine genomic profiling of patients with lung cancer, where in the USA it is routinely done for all patients and in Norway it is now done for all patients with advanced stages in connection with the IMPRESS-study (118).

6 Conclusion

This study reveals that KEAP1 mutation is the main driver of the immune desert phenotype in early stage lung adenocarcinoma compared to STK11 mutation. KEAP1 enrichment, either as a single mutation or co-mutation with STK11, leads to greater immune system suppression than STK11 mutation alone, as evidenced by the higher number of B-lymphocytes observed in STK11 mutated samples. Furthermore, the study suggests a possible link between KEAP1 mutation and chemoresistance in early stage lung adenocarcinoma. Future research should involve larger sample sizes and more diverse patient populations to validate these findings and investigate the underlying mechanisms. In the future, we are planning

for a complete examination of the data set with regard to the genes which were found to be associated with chemoresistance.

References

1. Sung H, Ferlay J, Siegel RL, Laversanne M, Soerjomataram I, Jemal A, et al. Global Cancer Statistics 2020: GLOBOCAN Estimates of Incidence and Mortality Worldwide for 36 Cancers in 185 Countries. CA Cancer J Clin. 2021;71(3):209-49.
2. Årsrapport 2021 med resultater og forbedringstiltak fra Nasjonalt kvalitetsregister for lungekreft. Oslo; 2021.
3. Årsrapport for lungekreft 2022. Oslo; 2023 10.05.
4. Helsedirektoratet. Cancer in Norway 2021. Oslo: Helsedirektoratet 2021.
5. Malhotra J, Malvezzi M, Negri E, La Vecchia C, Boffetta P. Risk factors for lung cancer worldwide. European Respiratory Journal. 2016;48(3):889-902.
6. Akhtar N, Bansal JG. Risk factors of Lung Cancer in nonsmoker. Current Problems in Cancer. 2017;41(5):328-39.
7. Witschi H. A Short History of Lung Cancer. Toxicological Sciences. 2001;64(1):4-6.
8. Agents classified by the IARC Monographs: WHO; 2022 [Available from: https://monographs.iarc.who.int/list-of-classifications.
9. Cheng ES, Weber M, Steinberg J, Yu XQ. Lung cancer risk in never-smokers: An overview of environmental and genetic factors. Chin J Cancer Res. 2021;33(5):548-62.
10. Matakidou A, Eisen T, Houlston R. Systematic review of the relationship between family history and lung cancer risk. British journal of cancer. 2005;93(7):825-33.
11. Hessol NA, LEVINE AM, MORRIS A, MARGOLICK JB, COHEN MH, JACOBSON LP, et al. Lung cancer incidence and survival among HIV-infected and uninfected women and men. AIDS (London, England). 2015;29(10):1183.
12. Zhai K, Ding J, Shi H-Z. HPV and lung cancer risk: a meta-analysis. Journal of Clinical Virology. 2015;63:84-90.
13. Conway EJ, Hudnall SD, Lazarides A, Bahler A, Fraire AE, Cagle PT. Absence of evidence for an etiologic role for Epstein-Barr virus in neoplasms of the lung and pleura. Modern Pathology: an Official Journal of the United States and Canadian Academy of Pathology, Inc. 1996;9(5):491-5.
14. Omenn GS, Goodman GE, Thornquist MD, Balmes J, Cullen MR, Glass A, et al. Effects of a combination of beta carotene and vitamin A on lung cancer and cardiovascular disease. New England journal of medicine. 1996;334(18):1150-5.
15. Woodson K, Tangrea JA, Barrett MJ, Virtamo J, Taylor PR, Albanes D. Serum α-tocopherol and subsequent risk of lung cancer among male smokers. Journal of the National Cancer Institute. 1999;91(20):1738-43.
16. Deneo-Pellegrini H, De Stefani E, Ronco A, Mendilaharsu M, Carzoglio JC. Meat consumption and risk of lung cancer; a case-control study from Uruguay. Lung Cancer. 1996;14(2-3):195-205.
17. Bagnardi V, Rota M, Botteri E, Tramacere I, Islami F, Fedirko V, et al. Alcohol consumption and site-specific cancer risk: a comprehensive dose–response meta-analysis. British journal of cancer. 2015;112(3):580-93.
18. Aldington S, Harwood M, Cox B, Weatherall M, Beckert L, Hansell A, et al. Cannabis use and risk of lung cancer: a case–control study. European Respiratory Journal. 2008;31(2):280-6.
19. Schabath MB, Cote ML. Cancer Progress and Priorities: Lung Cancer. Cancer Epidemiol Biomarkers Prev. 2019;28(10):1563-79.

20. Helsedirektoratet. Pakkeforløp på kreftområdet helsenorge.no: Helsedirektoratet 2016 [Available from: https://www.helsedirektoratet.no/nasjonale-forlop/generell-informasjon-for-alle-pakkeforlopene-for-kreft/pakkeforlop-pa-kreftomradet.
21. Helsedirektoratet. Nasjonalt handlingsprogram med retningslinjer for diagnostikk, behandling og oppfølging av lungekreft, mesoteliom og thymom. Oslo: Helsedirektoratet; 2023.
22. UNN. Regional kreftplan 2022-2026 2022 [78]. Available from: https://helse-nord.no/Documents/Høringer/2022%20Høring%20revidert%20regional%20kreftplan%20og%20delstrategi%20for%20kreft/Styresak%20112-2022%20Vedlegg%201.pdf.
23. Romaszko AM, Doboszyńska A. Multiple primary lung cancer: A literature review. Adv Clin Exp Med. 2018;27(5):725-30.
24. Thai AA, Solomon BJ, Sequist LV, Gainor JF, Heist RS. Lung cancer. The Lancet. 2021;398(10299):535-54.
25. Alberg AJ, Brock MV, Ford JG, Samet JM, Spivack SD. Epidemiology of Lung Cancer: Diagnosis and Management of Lung Cancer, 3rd ed: American College of Chest Physicians Evidence-Based Clinical Practice Guidelines. Chest. 2013;143(5, Supplement):e1S-e29S.
26. Detterbeck FC, Boffa DJ, Kim AW, Tanoue LT. The Eighth Edition Lung Cancer Stage Classification. Chest. 2017;151(1):193-203.
27. Lung Cancer - Non-Small Cell Guide: cancer.net 2022 [Available from: https://www.cancer.net/cancer-types/lung-cancer-non-small-cell.
28. Chevallier M, Borgeaud M, Addeo A, Friedlaender A. Oncogenic driver mutations in non-small cell lung cancer: Past, present and future. World J Clin Oncol. 2021;12(4):217-37.
29. Friedlaender A, Drilon A, Weiss GJ, Banna GL, Addeo A. KRAS as a druggable target in NSCLC: Rising like a phoenix after decades of development failures. Cancer Treat Rev. 2020;85:101978.
30. Trujillo JA, Sweis RF, Bao R, Luke JJ. T Cell-Inflamed versus Non-T Cell-Inflamed Tumors: A Conceptual Framework for Cancer Immunotherapy Drug Development and Combination Therapy Selection. Cancer Immunol Res. 2018;6(9):990-1000.
31. Kilvaer TK, Paulsen E-E, Andersen S, Rakaee M, Bremnes RM, Busund L-TR, et al. Digitally quantified CD8+ cells: the best candidate marker for an immune cell score in non-small cell lung cancer? Carcinogenesis. 2020;41(12):1671-81.
32. Stankovic B, Bjørhovde HAK, Skarshaug R, Aamodt H, Frafjord A, Müller E, et al. Immune Cell Composition in Human Non-small Cell Lung Cancer. Frontiers in Immunology. 2019;9.
33. Reuben A, Zhang J, Chiou SH, Gittelman RM, Li J, Lee WC, et al. Comprehensive T cell repertoire characterization of non-small cell lung cancer. Nat Commun. 2020;11(1):603.
34. Liu Y-T, Sun Z-J. Turning cold tumors into hot tumors by improving T-cell infiltration. Theranostics. 2021;11(11):5365-86.
35. Galon J, Bruni D. Approaches to treat immune hot, altered and cold tumours with combination immunotherapies. Nature Reviews Drug Discovery. 2019;18(3):197-218.
36. Donnem T, Kilvaer TK, Andersen S, Richardsen E, Paulsen EE, Hald SM, et al. Strategies for clinical implementation of TNM-Immunoscore in resected nonsmall-cell lung cancer. Annals of Oncology. 2016;27(2):225-32.

37. Sumbly V, Landry I. Unraveling the Role of STK11/LKB1 in Non-small Cell Lung Cancer. Cureus. 2022;14(1):e21078.
38. Wahl SGF, Dai HY, Emdal EF, Berg T, Halvorsen TO, Ottestad AL, et al. The Prognostic Effect of KRAS Mutations in Non-Small Cell Lung Carcinoma Revisited: A Norwegian Multicentre Study. Cancers (Basel). 2021;13(17).
39. Skoulidis F, Li BT, Dy GK, Price TJ, Falchook GS, Wolf J, et al. Sotorasib for Lung Cancers with KRAS p.G12C Mutation. N Engl J Med. 2021;384(25):2371-81.
40. Zyla RE, Hahn E, Hodgson A. Gene of the month: STK11. Journal of Clinical Pathology. 2021;74(11):681-5.
41. Shackelford DB, Shaw RJ. The LKB1-AMPK pathway: metabolism and growth control in tumour suppression. Nat Rev Cancer. 2009;9(8):563-75.
42. Wang Y-S, Chen J, Cui F, Wang H, Wang S, Hang W, et al. LKB1 is a DNA damage response protein that regulates cellular sensitivity to PARP inhibitors. Oncotarget. 2016;7(45).
43. Alessi DR, Sakamoto K, Bayascas JR. LKB1-dependent signaling pathways. Annu Rev Biochem. 2006;75:137-63.
44. Mograbi B, Heeke S, Hofman P. The Importance of STK11/LKB1 Assessment in Non-Small Cell Lung Carcinomas. Diagnostics. 2021;11(2):196.
45. Laderian B, Mundi P, Fojo T, E. Bates S. Emerging Therapeutic Implications of STK11 Mutation: Case Series. The Oncologist. 2020;25(9):733-7.
46. Kullmann L, Krahn MP. Controlling the master—upstream regulation of the tumor suppressor LKB1. Oncogene. 2018;37(23):3045-57.
47. Jansen M, Ten Klooster JP, Offerhaus GJ, Clevers H. LKB1 and AMPK family signaling: the intimate link between cell polarity and energy metabolism. Physiol Rev. 2009;89(3):777-98.
48. Faubert B, Vincent EE, Griss T, Samborska B, Izreig S, Svensson RU, et al. Loss of the tumor suppressor LKB1 promotes metabolic reprogramming of cancer cells via HIF-1α. Proceedings of the National Academy of Sciences. 2014;111(7):2554-9.
49. Sanchez-Cespedes M, Parrella P, Esteller M, Nomoto S, Trink B, Engles JM, et al. Inactivation of LKB1/STK11 Is a Common Event in Adenocarcinomas of the Lung1. Cancer Research. 2002;62(13):3659-62.
50. Collisson E. A. CJD, Chmielecki J. Comprehensive molecular profiling of lung adenocarcinoma. Nature. 2014;511(7511):543-50.
51. Ji H, Ramsey MR, Hayes DN, Fan C, McNamara K, Kozlowski P, et al. LKB1 modulates lung cancer differentiation and metastasis. Nature. 2007;448(7155):807-10.
52. Matsumoto S, Iwakawa R, Takahashi K, Kohno T, Nakanishi Y, Matsuno Y, et al. Prevalence and specificity of LKB1 genetic alterations in lung cancers. Oncogene. 2007;26(40):5911-8.
53. Kitajima S, Ivanova E, Guo S, Yoshida R, Campisi M, Sundararaman SK, et al. Suppression of STING Associated with LKB1 Loss in KRAS-Driven Lung Cancer. Cancer Discovery. 2019;9(1):34-45.
54. Della Corte CM, Byers LA. Evading the STING: LKB1 Loss Leads to STING Silencing and Immune Escape in KRAS-Mutant Lung Cancers. Cancer Discov. 2019;9(1):16-8.
55. Koyama S, Akbay EA, Li YY, Aref AR, Skoulidis F, Herter-Sprie GS, et al. STK11/LKB1 Deficiency Promotes Neutrophil Recruitment and Proinflammatory Cytokine Production to Suppress T-cell Activity in the Lung Tumor Microenvironment. Cancer Res. 2016;76(5):999-1008.

56. Di Federico A, De Giglio A, Parisi C, Gelsomino F. STK11/LKB1 and KEAP1 mutations in non-small cell lung cancer: Prognostic rather than predictive? European Journal of Cancer. 2021;157:108-13.
57. Shire NJ, Klein AB, Golozar A, Collins JM, Fraeman KH, Nordstrom BL, et al. STK11 (LKB1) mutations in metastatic NSCLC: Prognostic value in the real world. PLOS ONE. 2020;15(9):e0238358.
58. Skoulidis F, Goldberg ME, Greenawalt DM, Hellmann MD, Awad MM, Gainor JF, et al. STK11/LKB1 Mutations and PD-1 Inhibitor Resistance in KRAS-Mutant Lung Adenocarcinoma. Cancer Discovery. 2018;8(7):822-35.
59. Arbour KC, Riely GJ. Systemic Therapy for Locally Advanced and Metastatic Non-Small Cell Lung Cancer: A Review. Jama. 2019;322(8):764-74.
60. Facchinetti F, Bluthgen MV, Tergemina-Clain G, Faivre L, Pignon JP, Planchard D, et al. LKB1/STK11 mutations in non-small cell lung cancer patients: Descriptive analysis and prognostic value. Lung Cancer. 2017;112:62-8.
61. Best SA, De Souza DP, Kersbergen A, Policheni AN, Dayalan S, Tull D, et al. Synergy between the KEAP1/NRF2 and PI3K Pathways Drives Non-Small-Cell Lung Cancer with an Altered Immune Microenvironment. Cell Metabolism. 2018;27(4):935-43.e4.
62. Romero R, Sánchez-Rivera FJ, Westcott PMK, Mercer KL, Bhutkar A, Muir A, et al. Keap1 mutation renders lung adenocarcinomas dependent on Slc33a1. Nature Cancer. 2020;1(6):589-602.
63. Wohlhieter CA, Richards AL, Uddin F, Hulton CH, Quintanal-Villalonga À, Martin A, et al. Concurrent Mutations in STK11 and KEAP1 Promote Ferroptosis Protection and SCD1 Dependence in Lung Cancer. Cell Rep. 2020;33(9):108444.
64. Mitsuishi Y, Motohashi H, Yamamoto M. The Keap1–Nrf2 system in cancers: stress response and anabolic metabolism. Frontiers in Oncology. 2012;2.
65. Bai X, Chen Y, Hou X, Huang M, Jin J. Emerging role of NRF2 in chemoresistance by regulating drug-metabolizing enzymes and efflux transporters. Drug Metabolism Reviews. 2016;48(4):541-67.
66. McDonald JT, Kim K, Norris AJ, Vlashi E, Phillips TM, Lagadec C, et al. Ionizing Radiation Activates the Nrf2 Antioxidant Response. Cancer Research. 2010;70(21):8886-95.
67. Solis LM, Behrens C, Dong W, Suraokar M, Ozburn NC, Moran CA, et al. Nrf2 and Keap1 Abnormalities in Non–Small Cell Lung Carcinoma and Association with Clinicopathologic Features. Clinical Cancer Research. 2010;16(14):3743-53.
68. Xu X, Yang Y, Liu X, Cao N, Zhang P, Zhao S, et al. NFE2L2/KEAP1 Mutations Correlate with Higher Tumor Mutational Burden Value/PD-L1 Expression and Potentiate Improved Clinical Outcome with Immunotherapy. The Oncologist. 2020;25(6):e955-e63.
69. Barrera-Rodríguez R. Importance of the Keap1-Nrf2 pathway in NSCLC: Is it a possible biomarker? Biomed Rep. 2018;9(5):375-82.
70. Marinelli D, Mazzotta M, Scalera S, Terrenato I, Sperati F, D'Ambrosio L, et al. KEAP1-driven co-mutations in lung adenocarcinoma unresponsive to immunotherapy despite high tumor mutational burden. Annals of Oncology. 2020;31(12):1746-54.
71. Cristescu R, Mogg R, Ayers M, Albright A, Murphy E, Yearley J, et al. Pan-tumor genomic biomarkers for PD-1 checkpoint blockade–based immunotherapy. Science. 2018;362(6411):eaar3593.
72. Rakaee M, Andersen S, Giannikou K, Paulsen EE, Kilvaer TK, Busund LTR, et al. Machine learning-based immune phenotypes correlate with STK11/KEAP1 co-

mutations and prognosis in resectable NSCLC: a sub-study of the TNM-I trial. Annals of Oncology. 2023.
73. Sumii M, Namba M, Tokumo K, Yamauchi M, Okamoto W, Hattori N, et al. Concurrent Mutations in STK11 and KEAP1 Cause Treatment Resistance in KRAS Wild-type Non-small-cell Lung Cancer. Internal Medicine. 2023;advpub.
74. Lek M, Karczewski KJ, Minikel EV, Samocha KE, Banks E, Fennell T, et al. Analysis of protein-coding genetic variation in 60,706 humans. Nature. 2016;536(7616):285-91.
75. Landrum MJ, Lee JM, Benson M, Brown GR, Chao C, Chitipiralla S, et al. ClinVar: improving access to variant interpretations and supporting evidence. Nucleic Acids Res. 2018;46(D1):D1062-d7.
76. Kulkarni MM. Digital multiplexed gene expression analysis using the NanoString nCounter system. Curr Protoc Mol Biol. 2011;Chapter 25:Unit25B.10.
77. NanoString. nCounter® PanCancer IO 360™ Panel: NanoString; 2023 [Available from: https://nanostring.com/products/ncounter-assays-panels/oncology/pancancer-io-360/#signup.
78. ROSALIND. ROSALIND, a platform for learning bioinformatics through problem-solving 2023 [3.36.1.2:[Available from: www.rosalind.bio.
79. ROSALIND. How does ROSALIND QC my nCounter data? : Rosalind 2023 [Available from: https://www.rosalind.bio/en/knowledge/how-does-rosalind-qc-my-ncounter-data.
80. Wu Z, Liu W, Jin X, Ji H, Wang H, Glusman G, et al. NormExpression: An R Package to Normalize Gene Expression Data Using Evaluated Methods. Front Genet. 2019;10:400.
81. ROSALIND. How is my Gene Expression nCounter data normalized in ROSALIND? How does ROSALIND calculate differential expression for my Gene Expression nCounter data? : Rosalind; 2023 [Available from: https://www.rosalind.bio/en/knowledge/gene-expression-normalization-differential.
82. Perkins JR, Dawes JM, McMahon SB, Bennett DLH, Orengo C, Kohl M. ReadqPCR and NormqPCR: R packages for the reading, quality checking and normalisation of RT-qPCR quantification cycle (Cq) data. BMC Genomics. 2012;13(1):296.
83. Hennig C. Flexible Procedures for Clustering 2023 [Available from: https://cran.r-project.org/web/packages/fpc/index.html.
84. Liu J, Campen A, Huang S, Peng SB, Ye X, Palakal M, et al. Identification of a gene signature in cell cycle pathway for breast cancer prognosis using gene expression profiling data. BMC Med Genomics. 2008;1:39.
85. Itadani H, Mizuarai S, Kotani H. Can systems biology understand pathway activation? Gene expression signatures as surrogate markers for understanding the complexity of pathway activation. Curr Genomics. 2008;9(5):349-60.
86. Wikimedia Foundation I. Gene signature: Wikipedia, The Free Encyclopedia; 2023 [Available from: https://en.wikipedia.org/wiki/Gene_signature.
87. Gundersen GW, Jagodnik KM, Woodland H, Fernandez NF, Sani K, Dohlman AB, et al. GEN3VA: aggregation and analysis of gene expression signatures from related studies. BMC Bioinformatics. 2016;17(1):461.
88. Li M, Zhao J, Li X, Chen Y, Feng C, Qian F, et al. HiFreSP: A novel high-frequency sub-pathway mining approach to identify robust prognostic gene signatures. Brief Bioinform. 2020;21(4):1411-24.

89. Shafi A, Nguyen T, Peyvandipour A, Draghici S. GSMA: an approach to identify robust global and test Gene Signatures using Meta-Analysis. Bioinformatics. 2020;36(2):487-95.
90. NanoString. What is a GSA score and how is it interpreted? Seattle: NanoString 2023 [Available from: https://nanostring.com/support/knowledge-base-faqs/.
91. Wikimedia Foundation I. Gene set enrichment analysis: Wikipedia, The Free Encyclopedia; 2023 [Available from: https://en.wikipedia.org/wiki/Gene_set_enrichment_analysis.
92. Subramanian A, Tamayo P, Mootha VK, Mukherjee S, Ebert BL, Gillette MA, et al. Gene set enrichment analysis: a knowledge-based approach for interpreting genome-wide expression profiles. Proc Natl Acad Sci U S A. 2005;102(43):15545-50.
93. Mitchell AL, Attwood TK, Babbitt PC, Blum M, Bork P, Bridge A, et al. InterPro in 2019: improving coverage, classification and access to protein sequence annotations. Nucleic Acids Res. 2019;47(D1):D351-d60.
94. Geer LY, Marchler-Bauer A, Geer RC, Han L, He J, He S, et al. The NCBI BioSystems database. Nucleic Acids Res. 2010;38(Database issue):D492-6.
95. Liberzon A, Subramanian A, Pinchback R, Thorvaldsdóttir H, Tamayo P, Mesirov JP. Molecular signatures database (MSigDB) 3.0. Bioinformatics. 2011;27(12):1739-40.
96. Fabregat A, Jupe S, Matthews L, Sidiropoulos K, Gillespie M, Garapati P, et al. The Reactome Pathway Knowledgebase. Nucleic Acids Res. 2018;46(D1):D649-d55.
97. Slenter DN, Kutmon M, Hanspers K, Riutta A, Windsor J, Nunes N, et al. WikiPathways: a multifaceted pathway database bridging metabolomics to other omics research. Nucleic Acids Res. 2018;46(D1):D661-d7.
98. Yon Rhee S, Wood V, Dolinski K, Draghici S. Use and misuse of the gene ontology annotations. Nature Reviews Genetics. 2008;9(7):509-15.
99. Papillon-Cavanagh S, Doshi P, Dobrin R, Szustakowski J, Walsh AM. STK11 and KEAP1 mutations as prognostic biomarkers in an observational real-world lung adenocarcinoma cohort. ESMO Open. 2020;5(2):e000706.
100. Shen R, Martin A, Ni A, Hellmann M, Arbour KC, Jordan E, et al. Harnessing Clinical Sequencing Data for Survival Stratification of Patients with Metastatic Lung Adenocarcinomas. JCO Precis Oncol. 2019;3.
101. Quintero-Fabián S, Arreola R, Becerril-Villanueva E, Torres-Romero JC, Arana-Argáez V, Lara-Riegos J, et al. Role of Matrix Metalloproteinases in Angiogenesis and Cancer. Frontiers in Oncology. 2019;9.
102. Rundhaug JE. Matrix Metalloproteinases, Angiogenesis, and Cancer: Commentary re: A. C. Lockhart et al., Reduction of Wound Angiogenesis in Patients Treated with BMS-275291, a Broad Spectrum Matrix Metalloproteinase Inhibitor. Clin. Cancer Res., 9: 00–00, 2003. Clinical Cancer Research. 2003;9(2):551-4.
103. Gabrilovich DI, Nagaraj S. Myeloid-derived suppressor cells as regulators of the immune system. Nat Rev Immunol. 2009;9(3):162-74.
104. Mantovani A, Marchesi F, Malesci A, Laghi L, Allavena P. Tumour-associated macrophages as treatment targets in oncology. Nat Rev Clin Oncol. 2017;14(7):399-416.
105. Quail DF, Joyce JA. Microenvironmental regulation of tumor progression and metastasis. Nat Med. 2013;19(11):1423-37.
106. Talmadge JE, Gabrilovich DI. History of myeloid-derived suppressor cells. Nat Rev Cancer. 2013;13(10):739-52.

107. Condamine T, Ramachandran I, Youn JI, Gabrilovich DI. Regulation of tumor metastasis by myeloid-derived suppressor cells. Annu Rev Med. 2015;66:97-110.
108. Mantovani A. The growing diversity and spectrum of action of myeloid-derived suppressor cells. Eur J Immunol. 2010;40(12):3317-20.
109. Xia Y, Shen S, Verma IM. NF-κB, an active player in human cancers. Cancer Immunol Res. 2014;2(9):823-30.
110. Liu T, Zhang L, Joo D, Sun SC. NF-κB signaling in inflammation. Signal Transduct Target Ther. 2017;2:17023-.
111. Grivennikov SI, Greten FR, Karin M. Immunity, inflammation, and cancer. Cell. 2010;140(6):883-99.
112. Ward JP, Gubin MM, Schreiber RD. The Role of Neoantigens in Naturally Occurring and Therapeutically Induced Immune Responses to Cancer. Adv Immunol. 2016;130:25-74.
113. Evaristo C, Spranger S, Barnes SE, Miller ML, Molinero LL, Locke FL, et al. Cutting Edge: Engineering Active IKKβ in T Cells Drives Tumor Rejection. J Immunol. 2016;196(7):2933-8.
114. Hopewell EL, Zhao W, Fulp WJ, Bronk CC, Lopez AS, Massengill M, et al. Lung tumor NF-κB signaling promotes T cell-mediated immune surveillance. J Clin Invest. 2013;123(6):2509-22.
115. Zhang P, Singh A, Yegnasubramanian S, Esopi D, Kombairaju P, Bodas M, et al. Loss of Kelch-Like ECH-Associated Protein 1 Function in Prostate Cancer Cells Causes Chemoresistance and Radioresistance and Promotes Tumor GrowthThe Loss of Keap1 Activity in Prostate Cancer Cells. Molecular cancer therapeutics. 2010;9(2):336-46.
116. Yamadori T, Ishii Y, Homma S, Kurishima K, Minami Y, Noguchi M, et al. Resistance to chemotherapy in non-small cell lung cancer with Keap1 gene mutation. International Cancer Conference Journal. 2012;1(2):63-6.
117. Hung TH, Hsu SC, Cheng CY, Choo KB, Tseng CP, Chen TC, et al. Wnt5A regulates ABCB1 expression in multidrug-resistant cancer cells through activation of the non-canonical PKA/β-catenin pathway. Oncotarget. 2014;5(23):12273-90.
118. IMPRESS-Norway - clinical trial for cancer patients Oslo: OSLO UNIVERSITETSSYKEHUS HF; 2021 [Available from: https://impress-norway.no/en/impress-norway-front-page/.

Supplementary Figures

Figure S1: *Incidence of lung cancer by gender and age groups between 1992-2022 in Norway. Source: Annual report for the lung cancer registry 2022 (3).*

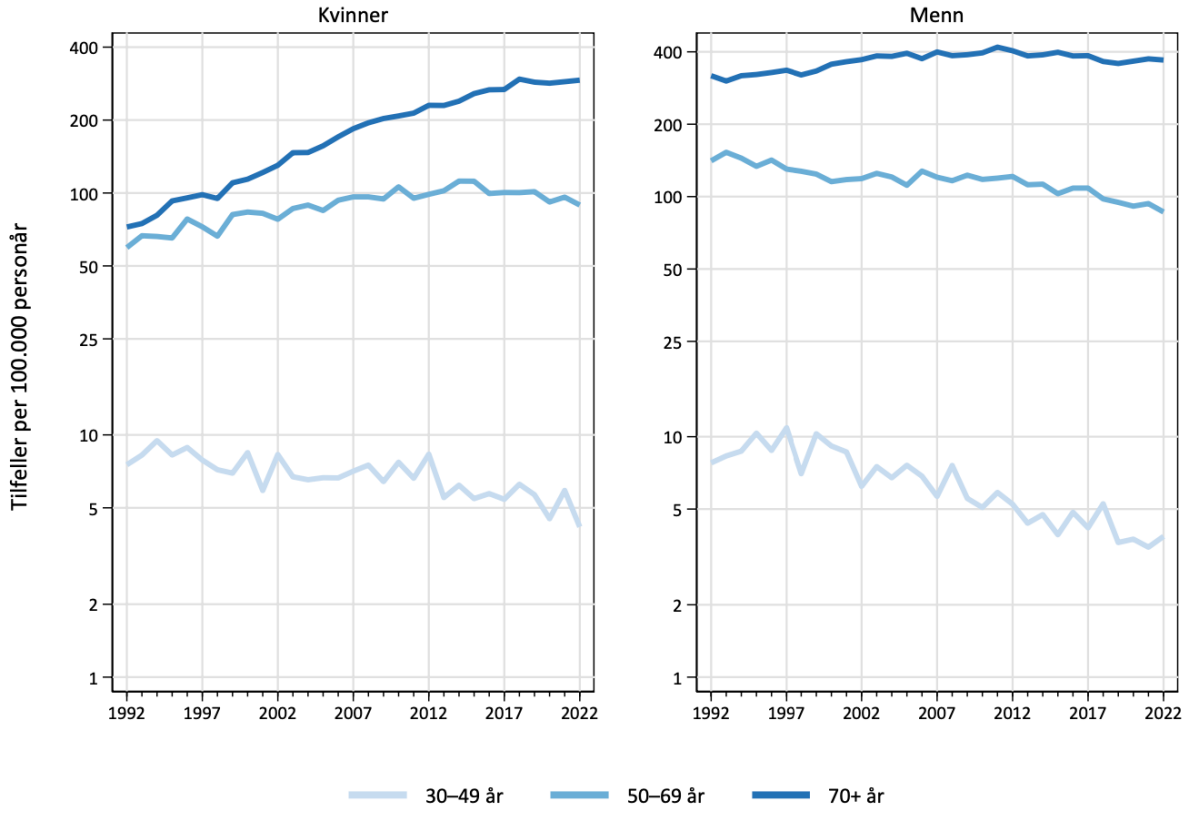

Figure S2 (left plot): shows the trend for men in incidence (dark blue), mortality (light blue) and 5-year relative survival (green) for lung cancer in the period 1965-2021. The **right plot** shows the trend for women in incidence (red), mortality (pink) and 5-year relative survival (brown) for lung cancer during the same period as for figure 2. *Source: the report Cancer in Norway 2021(4).*

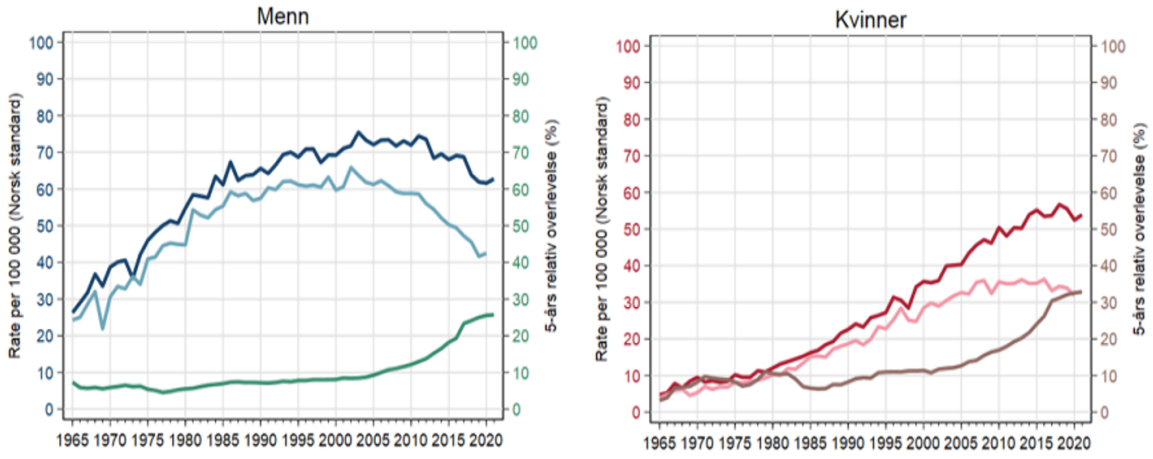

Figure S3: *Summary of investigation with diagnostic imaging and biopsy (21).*

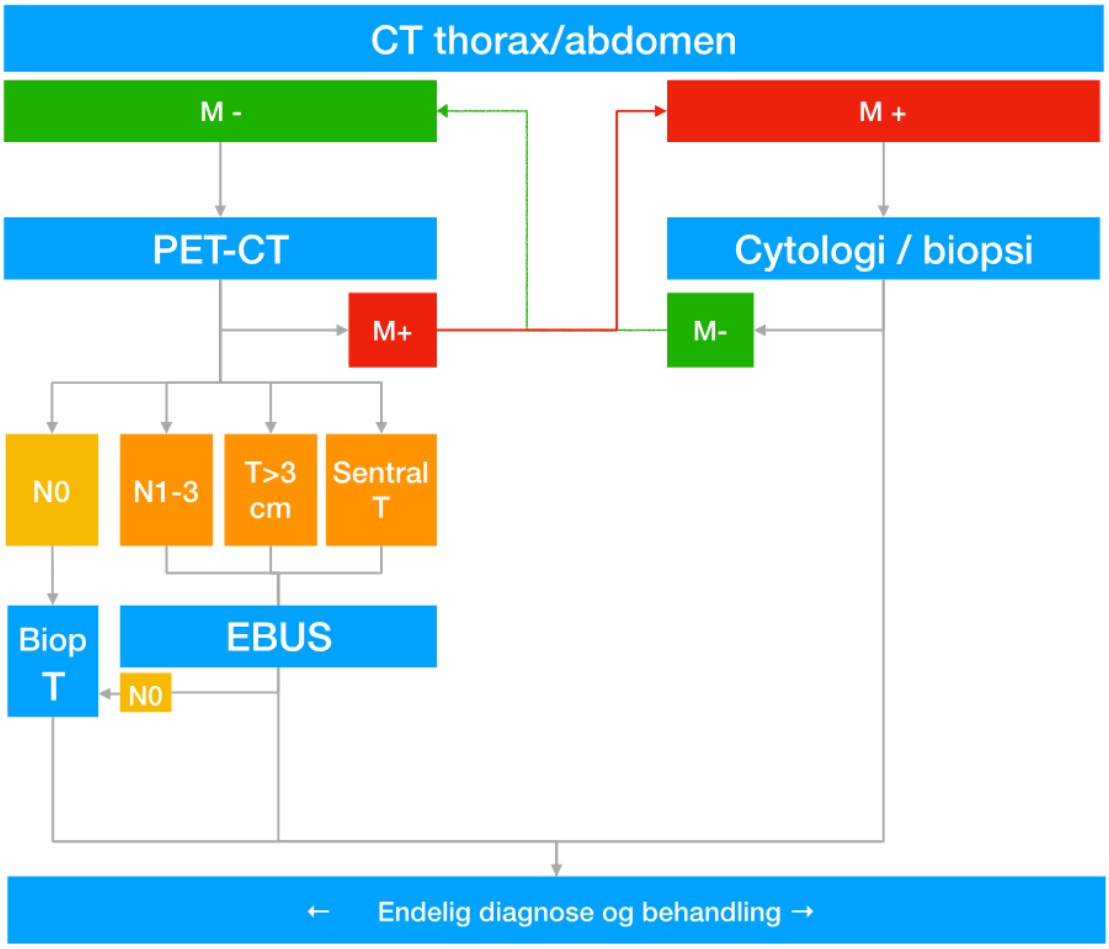

Figure S4: *Histological classification of lung cancer (19).*

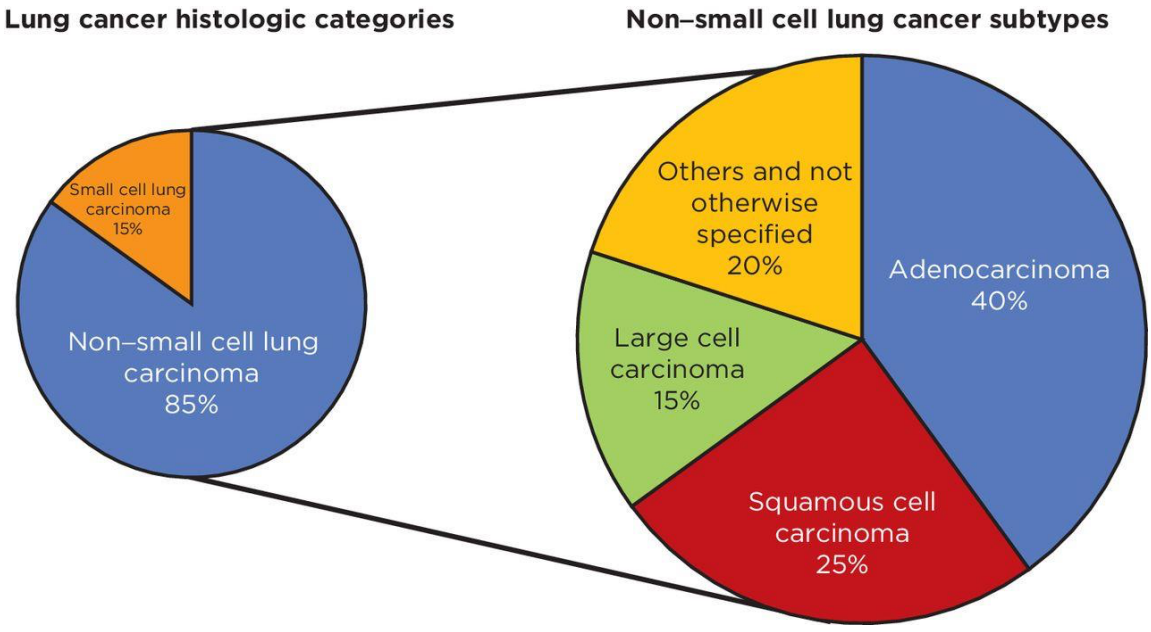

Figure S5: *Incidence of oncogenic drivers in non-small cell lung cancer (17).*

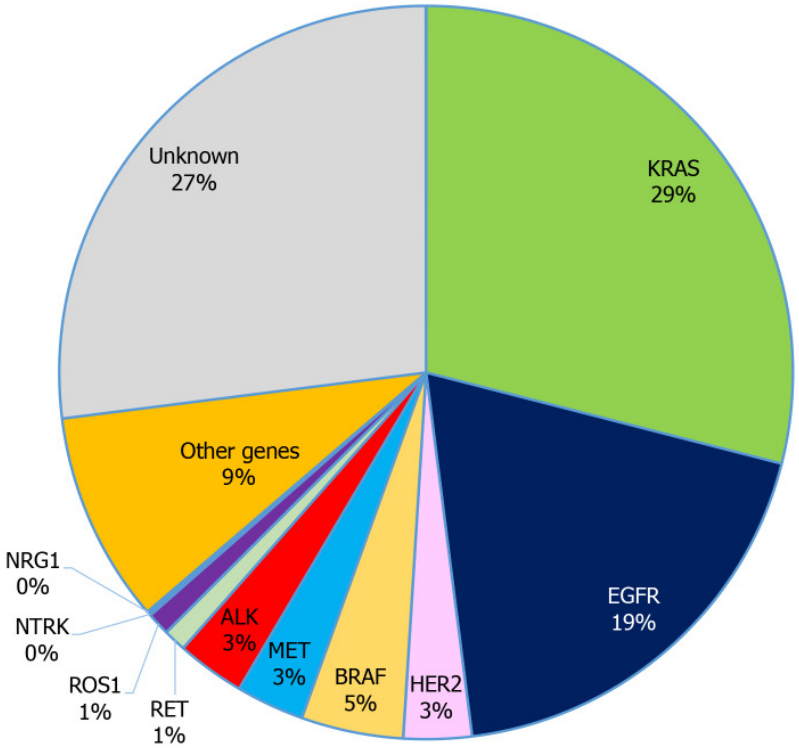

Figure S6: *Based on the spatial distribution of CD8+ T lymphocytes in the tumor microenvironment, a gradient of three immunophenotypes is observed: the immune-desert, immune-excluded and immune-inflamed phenotypes. In the immune-desert phenotype, immune cells are absent from the tumor and its periphery. In the immune-excluded phenotype, immune cells accumulate but do not efficiently infiltrate. In the immune-inflamed phenotype, immune cells infiltrate but their effects are inhibited. Notably, the three different phenotypes have different response rates to immune checkpoint inhibitors (34).*

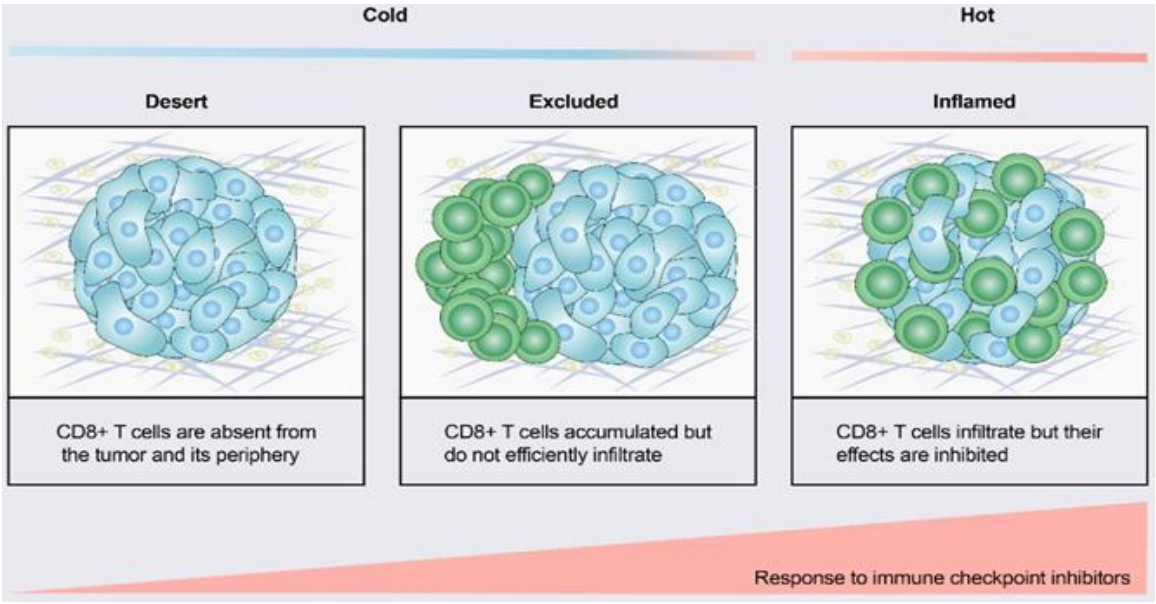

Figure S7: *An overview of nCounter workflow for gene expression assay (77)*

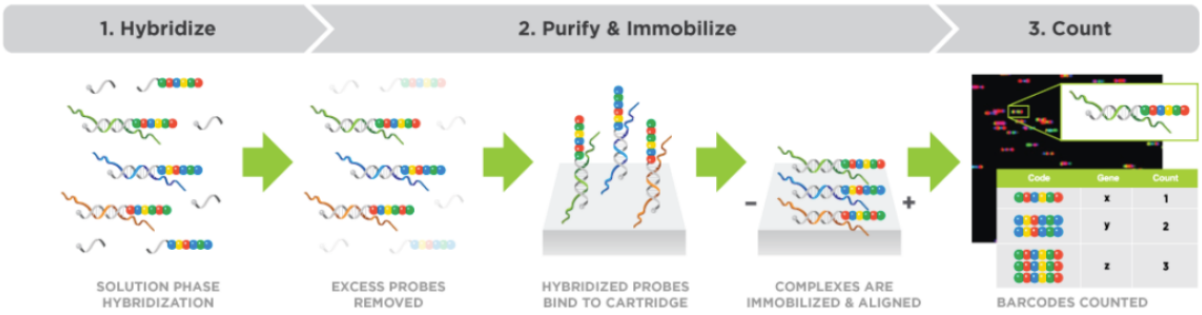

Supplementary Tables

Table S1: *Deadlines for the various parts of the guidelines for lung cancer in Norway (21).*

Tidsperiode	Behandlingstype	Antall kalenderdager
Fra henvisning mottatt til første fremmøte utredende avdeling		7
Fra første fremmøte i utredende avdeling til avsluttet utredning (beslutning tas)		21
Fra avsluttet utredning til start behandling	Kirurgisk behandling	14
Fra avsluttet utredning til start behandling	Medikamentell behandling	7
Fra avsluttet utredning til start behandling	Strålebehandling	14
Fra henvisning mottatt til start behandling	Kirurgisk behandling	42
Fra henvisning mottatt til start behandling	Medikamentell behandling	35
Fra henvisning mottatt til start behandling	Strålebehandling	42

Table S2: *The 8th edition of the TNM classification for non-small lung cancer (26).*

T (Primary Tumor)		**Label**
T0	No primary tumor	
Tis	Carcinoma in situ (Squamous or Adenocarcinoma)	Tis
T1	Tumor ≤3 cm,	
T1a(mi)	Minimally Invasive Adenocarcinoma	T1a*(mi)*
T1a	Superficial spreading tumor in central airways[a]	T1a *SS*
T1a	Tumor ≤1 cm	T1a *≤1*
T1b	Tumor >1 but ≤2 cm	T1b *>1-2*
T1c	Tumor >2 but ≤3 cm	T1c *>2-3*
T2	Tumor >3 but ≤5 cm or tumor involving:	
	visceral pleura[b],	T2 *Visc Pl*
	main bronchus (not carina), atelectasis to hilum[b]	T2 *Centr*
T2a	Tumor >3 but ≤4 cm	T2a *>3-4*
T2b	Tumor >4 but ≤5 cm	T2b *>4-5*
T3	Tumor >5 but ≤7 cm	T3 *>5--7*
	or invading chest wall, pericardium, phrenic nerve	T3 *Inv*
	or separate tumor nodule(s) in the same lobe	T3 *Satell*
T4	Tumor >7 cm	T4 *>7*
	or tumor invading: mediastinum, diaphragm, heart, great vessels, recurrent laryngeal nerve, carina, trachea, esophagus, spine;	T4 *Inv*
	or tumor nodule(s) in a different ipsilateral lobe	T4 *Ipsi Nod*
N (Regional Lymph Nodes)		
N0	No regional node metastasis	
N1	Metastasis in ipsilateral pulmonary or hilar nodes	
N2	Metastasis in ipsilateral mediastinal/subcarinal nodes	
N3	Metastasis in contralateral mediastinal/hilar, or supraclavicular nodes	
M (Distant Metastasis)		
M0	No distant metastasis	
M1a	Malignant pleural/pericardial effusion[c] or pleural /pericardial nodules	M1a *Pl Dissem*
	or separate tumor nodule(s) in a contralateral lobe;	M1a *Contr Nod*
M1b	Single extrathoracic metastasis	M1b *Single*
M1c	Multiple extrathoracic metastases (1 or >1 organ)	M1c *Multi*

Table S3: *QC metrics for the 23 samples that were included in the study.*

Sample name	Sample ID	FOV total	FOV counted	Imaging quality (%FOV captured)	Binding density	Positive control linearity	meanOfNegativeControls	standardDeviationOfNegControls	positiveControlE	positiveControlA	housekeepingGenesAbove50
20191022_TNMI-2ND_01_01.RCC	1777726	555	499	0.899099	0.98	1.0	18.88	6.98	147.0	44254.0	100.0
20191022_TNMI-2ND_06_03.RCC	1777727	555	528	0.951351	0.54	0.99	18.25	6.76	199.0	55451.0	100.0
20191022_TNMI-2ND_25_09.RCC	1777728	555	534	0.962162	0.84	0.99	16.5	6.19	144.0	38397.0	100.0
20200210_TNMI3_33_01.RCC	1777729	555	514	0.926126	0.94	0.99	9.75	3.77	87.0	26201.0	100.0
20200210_TNMI3_71_10.RCC	1777730	555	537	0.967568	0.73	0.99	12.88	7.59	145.0	42142.0	100.0
20200211_TNMI4_57_02.RCC	1777731	555	533	0.96036	1.35	0.99	16.0	5.04	113.0	34344.0	100.0
20200228_TNMI6_52B2_10.RCC	1777732	555	515	0.927928	1.31	0.99	18.25	2.92	106.0	30096.0	100.0
20200928_TNMI260-2_3-1_07.RCC	1777733	555	519	0.935135	1.01	0.99	27.38	12.69	140.0	39776.0	100.0
20200928_TNMI260-2_3-6_11.RCC	1777734	555	536	0.965766	0.44	0.96	8.88	4.82	76.0	15709.0	100.0
20200928_TNMI260-2_32_03.RCC	1777735	555	545	0.981982	0.81	0.99	27.75	10.1	200.0	50408.0	100.0
20201005_TNMI260-3_3-11_04.RCC	1777736	555	545	0.981982	0.78	0.99	18.88	7.51	129.0	40890.0	100.0
20201005_TNMI260-3_3-13_06.RCC	1777737	555	546	0.983784	0.78	0.99	17.62	3.85	120.0	31342.0	100.0
20201005_TNMI260-3_3-14_07.RCC	1777738	555	549	0.989189	0.89	0.98	20.62	7.95	105.0	35538.0	100.0
20201012_TNMI260-4_3-3_01.RCC	1777739	555	540	0.972973	0.4	0.99	27.38	9.12	222.0	71424.0	100.0
20201014_TNMI260-5_6-6_08.RCC	1777740	555	521	0.938739	1.22	0.99	22.25	8.73	162.0	45597.0	100.0
20201014_TNMI260-5_6-12_12.RCC	1777741	555	534	0.962162	1.09	1.0	22.12	7.74	198.0	56843.0	100.0
20201020_TNMI260-8_7-24_05.RCC	1777742	555	537	0.967568	0.93	0.99	20.88	6.94	163.0	48070.0	100.0
20201023_TNMI260-9_7-38_02.RCC	1777743	555	537	0.967568	0.96	1.0	26.25	9.08	270.0	75007.0	100.0
20201023_TNMI260-9_7-46_07.RCC	1777744	555	541	0.974775	0.96	1.0	33.12	10.48	293.0	82645.0	100.0
20201023_TNMI260-9_7-49_09.RCC	1777745	555	523	0.942342	1.41	0.99	28.12	8.13	196.0	58390.0	100.0
20201027_TNMI260-10_7-53_01.RCC	1777746	555	535	0.963964	1.05	0.99	23.0	6.32	146.0	48796.0	100.0
20201027_TNMI260-10_7-61_04.RCC	1777747	555	534	0.962162	1.0	0.99	19.25	7.21	135.0	43501.0	100.0
20201027_TNMI260-10_7-77_09.RCC	1777748	555	535	0.963964	0.65	0.99	20.38	8.4	185.0	52233.0	100.0

Table S4: *The table contains various parameters for the PanglaoDB Cell Types pathways for STK11 vs. co-mutation, where the table is sorted by descending FDR-adjusted p-Value with the most significant p-values at the top.*

Cell Type	FDR-adjusted p-Value	# of Genes in Term	# of Genes that are also in this Filter or Cluster	# of Up-regulated genes	# of Down-regulated genes
B cells	0,01489	47	10	10	0
B cells memory	0,11801	66	10	10	0
Pancreatic stellate cells	0,11801	19	4	4	0
Thymocytes	0,11801	22	7	7	0
NK cells	0,17917	77	14	14	0
T cells	0,20791	49	11	11	0
B cells naive	0,29274	66	8	8	0
Cajal-Retzius cells	0,33113	6	2	2	0
Macrophages	0,33647	126	16	15	1
Adipocytes	0,36748	103	3	3	0
Basophils	0,36748	73	5	5	0
Cholangiocytes	0,36748	42	2	2	0
Ductal cells	0,36748	42	2	2	0

Table S5: *The table contains various parameters for the MSigDB Biological Process pathways for STK11 vs. co-mutation, where the table is sorted by descending FDR-adjusted p-Value with the most significant p-values at the top.*

Term name	FDR-adjusted p-Value	# of Genes in Term	# of Genes that are also in this Filter or Cluster	# of Up-regulated genes	# of Down-regulated genes
GO_CELL_ACTIVATION	0.00074	1423	73	70	3
GO_B_CELL_ACTIVATION	0.03088	300	25	24	1
GO_LYMPHOCYTE_ACTIVATION	0.05447	720	52	50	2
GO_CELL_ACTIVATION_INVOLVED_IN_IMMUNE_RESPONSE	0.07243	704	35	35	0
GO_SUBSTRATE_ADHESION_DEPENDENT_CELL_SPREADING	0.08407	87	5	5	0
GO_LYMPHOCYTE_DIFFERENTIATION	0.10396	347	32	31	1
GO_REGULATION_OF_B_CELL_ACTIVATION	0.14357	179	16	16	0
GO_EXOCYTOSIS	0.14357	899	27	27	0
GO_B_CELL_RECEPTOR_SIGNALING_PATHWAY	0.14357	120	9	9	0
GO_LIPOPROTEIN_METABOLIC_PROCESS	0.20772	29	4	4	0
GO_ADAPTIVE_IMMUNE_RESPONSE	0.20772	620	36	36	0
GO_REGULATION_OF_LYMPHOCYTE_ACTIVATION	0.20772	477	36	36	0
GO_REGULATION_OF_LYMPHOCYTE_DIFFERENTIATION	0.20963	168	18	18	0

Table S6: *The table contains various parameters for the MSigDB Reactome pathways for KEAP1 vs. co-mutation, where the table is sorted by descending FDR-adjusted p-Value with the most significant p-values at the top.*

Term Name	FDR-adjusted p-Value	# of Genes in Term	# of Genes in Term	# of Up-regulated genes
REACTOME ACTIVATION OF MATRIX METALLOPROTEINASES	0.00695	33	2	2
REACTOME DEGRADATION OF THE EXTRACELLULAR MATRIX	0.03771	140	2	2
REACTOME EXTRACELLULAR MATRIX ORGANIZATION	0.03771	301	3	3
REACTOME COLLAGEN FORMATION	0.03771	90	2	2
REACTOME COLLAGEN DEGRADATION	0.03771	64	2	2
REACTOME ASSEMBLY OF COLLAGEN FIBRILS AND OTHER MULTIMERIC STRUCTURES	0.03771	61	2	2
REACTOME EXTRA NUCLEAR ESTROGEN SIGNALING	0.03771	75	2	2
REACTOME ESR MEDIATED SIGNALING	0.05737	219	2	2
REACTOME SIGNALING BY NUCLEAR RECEPTORS	0.05737	262	2	2
REACTOME WNT5A DEPENDENT INTERNALIZATION OF FZD4	0.06201	15	1	1

Table S7: *The table contains various parameters for the MSigDB - Chemical and Genetic Perturbations pathways for KEAP1 vs. co-mutation, where the table is sorted by descending FDR-adjusted p-value with the most significant p-values at the top. The mentioned pathway in the main text is highlighted in light gray in the table.*

Term ID	FDR-adjusted p-Value	# of Genes in Term	# of Genes that are also in this Filter or Cluster	# of Up-regulated genes	# of Down-regulated genes
TAKEDA_TARGETS_OF_NUP98_HOXA9_FUSION_6HR_UP	0.07837	86	2	2	0
HERNANDEZ_MITOTIC_ARREST_BY_DOCETAXEL_1_UP	0.07837	35	2	2	0
TSUNODA_CISPLATIN_RESISTANCE_DN	0.07837	50	2	2	0
WANG_HCP_PROSTATE_CANCER	0.07837	105	2	2	0
LU_TUMOR_VASCULATURE_UP	0.08492	29	1	1	0
DAVICIONI_PAX_FOXO1_SIGNATURE_IN_ARMS_UP	0.08492	60	1	1	0
CHEMNITZ_RESPONSE_TO_PROSTAGLANDIN_E2_DN	0.08492	389	2	2	0
TURASHVILI_BREAST_DUCTAL_CARCINOMA_VS_DUCTAL_NORMAL_DN	0.08492	200	2	2	0
TURASHVILI_BREAST_DUCTAL_CARCINOMA_VS_LOBULAR_NORMAL_DN	0.08492	70	1	1	0
TURASHVILI_BREAST_LOBULAR_CARCINOMA_VS_DUCTAL_NORMAL_DN	0.08492	91	1	1	0
ZHOU_INFLAMMATORY_RESPONSE_LIVE_UP	0.08492	441	2	2	0
ZHOU_INFLAMMATORY_RESPONSE_LIVE_DN	0.08492	376	1	1	0
HOOI_ST7_TARGETS_DN	0.08492	117	1	1	0

Table S8: *The table contains various parameters for the PanglaoDB Cell Types pathways for STK11 vs. KEAP1, where the table is sorted by descending FDR-adjusted p-value with the most significant p-values at the top.*

Cell Type	FDR-adjusted p-Value	# of Genes in Term	# of Genes that are also in this Filter or Cluster	# of Up-regulated genes	# of Down-regulated genes
Astrocytes	0,22005	62	2	0	2
B cells	0,22005	47	3	3	0
B cells memory	0,22005	66	3	3	0
B cells naive	0,22005	66	2	2	0
Cajal-Retzius cells	0,22005	6	1	1	0
Cardiac stem and precursor cells	0,22005	8	1	0	1
Follicular cells	0,22005	8	1	1	0
Glomus cells	0,22005	28	1	0	1
Interneurons	0,22005	49	1	1	0
Leydig cells	0,22005	36	1	1	0
Luteal cells	0,22005	3	1	1	0
Mammary epithelial cells	0,22005	28	1	1	0
Megakaryocytes	0,22005	48	3	2	1
Neural stem/precursor cells	0,22005	27	2	0	2

Table S9: *The table gives an overview of the various Panther pathways for the comparison between STK11 vs. KEAP1, where the table is sorted by descending FDR-adjusted p-value with the most significant p-value at the top. In addition, the box on the right shows the up-regulated genes in the "B cell activation" pathways, where they are again sorted by decreasing FC (Log2 FC).*

Term Name	p-Value	FDR-adjusted p-Value	Number of Genes in Term	Number of Genes that are also in this Filter or Cluster	Number of Up-regulated genes	Number of Down-regulated genes
B cell activation	0.00620	0.18602	57	4	4	0
Ubiquitin proteasome pathway	0.14973	0.46239	43	1	0	1
Cell cycle	0.14973	0.46239	16	1	0	1
Axon guidance mediated by netrin	0.31699	0.46239	30	1	1	0
Integrin signalling pathway	0.46239	0.46239	156	2	1	1
Endothelin signaling pathway	0.45312	0.46239	75	1	1	0
Ras Pathway	0.42169	0.46239	69	1	1	0
PDGF signaling pathway	0.36418	0.46239	112	2	2	0
Interleukin signaling pathway	0.19933	0.46239	86	3	2	1
Insulin/IGF pathway-protein kinase B signaling cascade	0.38858	0.46239	34	1	1	0
Hypoxia response via HIF activation	0.42169	0.46239	24	1	1	0
p53 pathway feedback loops 2	0.28246	0.46239	45	2	1	1
p53 pathway	0.36418	0.46239	71	2	1	1
Notch signaling pathway	0.38858	0.46239	38	1	1	0
Glycolysis	0.31699	0.46239	17	1	0	1
Fructose galactose metabolism	0.19480	0.46239	10	1	0	1
T cell activation	0.48118	0.48118	72	2	2	0
PI3 kinase pathway	0.48295	0.48295	42	1	0	1
Inflammation mediated by chemokine and cytokine signaling pathway	0.49049	0.49049	188	3	3	0
TGF-beta signaling pathway	0.53811	0.53811	88	1	1	0
VEGF signaling pathway	0.53811	0.53811	54	1	1	0
FGF signaling pathway	0.53811	0.53811	99	1	1	0
Apoptosis signaling pathway	0.61808	0.61808	102	2	2	0
Angiogenesis	0.63337	0.63337	142	2	1	1
Cadherin signaling pathway	0.65293	0.65293	150	1	0	1
Alzheimer disease-presenilin pathway	0.69090	0.69090	99	1	0	1
Toll receptor signaling pathway	0.70839	0.70839	49	1	1	0
EGF receptor signaling pathway	0.70839	0.70839	109	1	1	0
Wnt signaling pathway	0.84873	0.84873	278	1	0	1
CCKR signaling map ST	0.86617	0.86617	165	1	1	0